Prepared for submission to JHEP TIF-UNIMI-2016-10

Precision Measurement of the W–Boson Mass: Theoretical Contributions and Uncertainties

Carlo Michel Carloni Calame,[a] **Mauro Chiesa ,**[a,1] **Homero Martinez,**[b] **Guido Montagna,**[b] **Oreste Nicrosini,**[a] **Fulvio Piccinini,**[a] **Alessandro Vicini**[c]

[a] *INFN, Sezione di Pavia, Via A. Bassi 6, 27100, Pavia, Italy*

[b] *Dipartimento di Fisica, Università di Pavia, and INFN, Sezione di Pavia, Via A. Bassi 6, 27100, Pavia, Italy*

[c] *Tif lab, Dipartimento di Fisica, Università di Milano, and INFN, Sezione di Milano, Via G. Celoria 16, 20133, Milano, Italy*

arXiv:1612.02841v1 [hep-ph] 8 Dec 2016

Abstract: We perform a comprehensive analysis of electroweak, QED and mixed QCD-electroweak corrections underlying the precise measurement of the W-boson mass M_W at hadron colliders. By applying a template fitting technique, we detail the impact on M_W of next-to-leading order electroweak and QCD corrections, multiple photon emission, lepton pair radiation and factorizable QCD-electroweak contributions. As a by-product, we provide an up-to-date estimate of the main theoretical uncertainties of perturbative nature. Our results can serve as a guideline for the assessment of the theoretical systematics at the Tevatron and LHC and allow a more robust precision measurement of the W-boson mass at hadron colliders.

Keywords: W–boson mass, hadron colliders, electroweak corrections, QED radiation, lepton pairs, mixed QCD-electroweak corrections, theoretical uncertainty

[*] Present address: Julius-Maximilians-Universität Würzburg, Institut für Theoretische Physik und Astrophysik, D-97074 Würzburg, Germany.

Contents

1 Introduction **2**

2 Theoretical and experimental framework **3**
- 2.1 Existing calculations and simulation codes 3
- 2.2 Classification of theoretical uncertainties 4
  - 2.2.1 Non-perturbative effects: PDFs and $p_\perp^W$ modeling 4
  - 2.2.2 EW and QED uncertainties: the Tevatron approach 5
  - 2.2.3 Mixed QCD-EW corrections 6

3 Theoretical tools **7**
- 3.1 The HORACE-3.1 formulation 7
- 3.2 Lepton-pair corrections in HORACE-3.1 9
- 3.3 POWHEG with QCD and EW corrections 11
  - 3.3.1 POWHEG-V2 `two-rad` improved version for DY processes 12

4 Perturbative uncertainties **14**
- 4.1 EW input scheme 14
- 4.2 Mixed $\mathcal{O}(\alpha\alpha_s)$ corrections 17

5 Impact of radiative corrections on the kinematical distributions **18**
- 5.1 Light lepton pairs radiation 19
- 5.2 QED FSR modeling 19
- 5.3 QCD corrections and QCD-QED interplay 21
- 5.4 Mixed QCD-EW corrections 23

6 Impact of radiative corrections on the M_W determination **25**
- 6.1 Template fitting method and simulation details 25
- 6.2 QED, EW and lepton-pair corrections 27
- 6.3 EW input scheme variation 29
- 6.4 Mixed QCD-EW corrections 30
  - 6.4.1 Comparisons with fixed-order results 31
  - 6.4.2 Results for the Tevatron 33
  - 6.4.3 Results for the LHC 35
  - 6.4.4 Impact on M_W determination of the POWHEG-V2 `two-rad` improvement 38

7 Conclusions **39**

A Appendix: PHOTOS setup **41**

B Appendix: Lepton-pair radiation **41**

1 Introduction

The high-precision measurement of the W-boson mass (M_W) offers the possibility of a stringent test of the Standard Model (SM) of the electroweak (EW) and strong interactions. The recent results by the Tevatron collaborations CDF ($M_W = 80.387 \pm 0.019$ GeV) [1] and DØ ($M_W = 80.375 \pm 0.023$ GeV) [2–4] dominate the current world average ($M_W = 80.385 \pm 0.015$ GeV) [5], which has now an accuracy of $2 \cdot 10^{-4}$. Also the LHC experiments ATLAS and CMS are planning to measure M_W and the possibility of reaching a final error of 15 MeV or eventually of 10 MeV has been discussed [6–8].

The SM prediction for M_W has been reevaluated in ref. [9] ($M_W = 80.357 \pm 0.009 \pm 0.003$ GeV), including the full 2-loop EW corrections derived from the study of the muon-decay amplitude, the leading 3-loop QCD effects and some classes of loop corrections to all orders. The two main sources of error in the theoretical predictions are the parametric uncertainty induced by the top quark mass value and the effect of missing higher orders, with similar importance in the final result. The comparison of the experimental world average with the SM prediction, in a global fit of the EW parameters that includes, among others, the top and the Higgs boson masses, is of primary importance to appreciate possible tensions in the SM [10]. Furthermore, in case of a significant discrepancy, it might be possible to derive some indirect hints of physics beyond the SM [11]. For this reason, it is crucial to have control on all the contributions to the final systematic error of the experimental result, both of experimental and theoretical origin.

The W-boson mass is measured at hadron colliders from the analysis of the distributions of the kinematic variables of the final state leptons of the charged current (CC) Drell-Yan (DY) process ($p\overset{(-)}{p} \to l\nu_l + X$, $l = e, \mu$). The lepton-pair transverse mass, the charged lepton transverse momentum and the missing transverse momentum distributions have a jacobian enhancement that makes them sensitive to the precise value of M_W. The measurement of the latter is derived from the accurate knowledge of the shape of these differential cross sections, via a template fit procedure.

The templates are computed with Monte Carlo simulations that include higher-order radiative corrections and that allow to account for the acceptance cuts and for the response of the detector. Each element of the simulation may affect the basic shape of the distributions and in turn have an impact on the central value extracted from the fitting procedure. The whole approach requires *i*) the discussion of the effects that are available as well as those that are not included in the preparation of the templates and *ii*) the propagation onto the M_W determination of the uncertainties affecting each of the elements entering in the Monte Carlo simulation.

The goals of the paper are the following. First, we assess the impact on the M_W determination due to different subsets of EW corrections which are presently available in public simulation codes. However, since we want to focus on the impact of the EW

corrections on the DY observables relevant to measure M_W at hadron colliders, we also need to consider their interplay with the QCD description of the process. Secondly, we estimate the impact of missing higher-order EW and mixed QCD-EW corrections, which are among the sources of theoretical uncertainty in the M_W measurement.

To achieve these goals, we developed an improved version of the EW Monte Carlo program HORACE-3.1, to study the impact of EW input scheme variations and simulate the radiation of light lepton pairs. Along the lines described in Ref. [12], we also implemented a new version of the POWHEG-V2 generator (named POWHEG-V2 `two-rad` in the following) for the simulation of DY processes in the presence of both QCD and EW corrections.

The paper is organized as follows. After a discussion of the main aspects of the theoretical and experimental framework in which the M_W measurement is performed (section 2), we describe in section 3 the theoretical and computational features of the tools used in our study. In section 4 we briefly discuss the uncertainties induced by $\mathcal{O}(\alpha^2)$ EW corrections (EW input scheme) and $\mathcal{O}(\alpha\alpha_s)$ corrections. Section 5 and section 6 are devoted to the presentation and discussion of our numerical results. In section 5 we detail the impact of various sources of higher-order corrections on the differential cross sections used to extract M_W from the data, while in section 6 we quantify the M_W shifts by the same higher-order contributions. Results for both the Tevatron and the LHC are given. Our conclusions are drawn in section 7.

2 Theoretical and experimental framework

2.1 Existing calculations and simulation codes

The DY processes start at Leading Order (LO) with purely EW amplitudes and receive radiative corrections that are exactly known up to $\mathcal{O}(\alpha_s^2)$ [13–17] in the strong interaction coupling, and that are implemented, at fully differential level with respect to the leptonic variables, in codes like FEWZ [18], DYNNLO [19], MCFM [20] and SHERPA [21]. The N^{3}LO threshold corrections for the inclusive cross section and for the rapidity distributions of the dilepton pair have been presented in refs. [22, 23]. The corrections up to $\mathcal{O}(\alpha)$ [24–27] in the EW coupling are also available and are implemented in different public codes like WZGRAD [25, 26, 28, 29], RADY [27, 30], SANC [31–33], HORACE-3.1 [34, 35]. A systematic overview and comparison among different codes for DY simulations have been presented in ref. [36].

Fixed-order results are not sufficient to reach the level of accuracy needed for a precise measurement of M_W. The approximated inclusion of multiple parton initial state radiation (ISR) to all perturbative orders is necessary to obtain a sensible description of the lepton-pair transverse momentum distribution and is known up to next-to-next-to-leading logarithmic (NNLL) QCD accuracy [37, 38] with respect to the $L_{\rm QCD} \equiv \log(p_\perp^V/m_V)$ factor, where $p_\perp^V$ is the lepton-pair transverse momentum and m_V is the relevant gauge boson mass ($V = W, Z$); these corrections have been implemented in simulation codes like RESBOS [39] or DYQT/DYRES [40, 41]. The inclusion of multiple photon radiation effects is necessary to achieve an accurate description of the leptonic observables, it is known up to leading-logarithmic (LL) accuracy with respect to the $L_{\rm QED} \equiv \log(\hat{s}/m_l^2)$

enhancement factor, where $\hat{s}$ is the partonic Mandelstam variable and m_l is the final state lepton mass; these corrections are available in codes like PHOTOS or HORACE-3.1 [42–46]. The problem of merging fixed-order and all-order results, avoiding double counting, has been separately discussed in QCD [21, 39, 47–51] and in the EW SM [34, 52]. QCD and EW results have to be combined together to obtain a realistic description of the DY final states: general purpose Shower Monte Carlo programs, like PYTHIA[53, 54], HERWIG[55] or SHERPA[56], include the possibility of multiple photon, gluon and quark emissions via a combined application of QCD and QED Parton Shower (PS), retaining only LL accuracy in the respective large logarithmic factors. In the absence of an exact calculation of the first mixed $\mathcal{O}(\alpha\alpha_s)$ corrections, several recipes have been devised to include the bulk of the two sets of effects including factorizable subleading effects both of QCD and EW origin [57–62], and preserving the NLO-QCD and NLO-EW accuracy on the quantities inclusive with respect to additional radiation [63–65].

2.2 Classification of theoretical uncertainties

The value of M_W is extracted with a template fit technique. The templates are theoretical distributions of the relevant observables, prepared with Monte Carlo simulation codes and keeping M_W as a free parameter; the accuracy of all the elements that enter in these codes has a direct impact on the final accuracy of the M_W determination. According to the factorized formulation of the hadron level cross section, we can identify two groups of effects as main sources of theoretical uncertainty: *i*) the non-perturbative effects stemming from the the proton description at low transverse momentum scales (probability density functions (PDFs), lepton-pair transverse momentum ($p_\perp^W$) modeling, intrinsic transverse momentum of the partons in the proton) and *ii*) the perturbative radiative corrections (QCD, EW, mixed QCD-EW) to the partonic cross section.

2.2.1 Non-perturbative effects: PDFs and $p_\perp^W$ modeling

The knowledge of the structure of the proton in terms of elementary constituents (quarks, gluons, photons) is affected by different uncertainties stemming at low-momentum scales, where QCD non-perturbative effects are important.

The proton collinear PDFs suffer of the errors of the experimental data from which they are extracted; these uncertainties are represented by the PDF collaborations with sets of replicas that have to be used to propagate the PDF error to the observables under study. These replicas are parametrizations of the proton structure equally compatible with the data, with a given confidence level; they are all on the same footing for the preparation of the templates used to fit M_W. The CDF and DØ collaborations have used the PDF set CTEQ6M to estimate the corresponding uncertainty on M_W and reported respectively a PDF contribution of 10 MeV [1] and of 11 MeV [2] to the systematic error. An extensive survey on the PDF uncertainties on M_W, considering different sets of global PDFs whose results are then combined according to the PDF4LHC recipe [66], has been performed at generator level (i.e. without including the effects of the detector response) in refs. [67–71].

The prediction of the lepton-pair transverse momentum distribution requires, in the limit $p_\perp^W \to 0$, the resummation to all orders of perturbative corrections which are logarith-

mically divergent. In the region of small $p_\perp^W$ there might be non-perturbative contributions to the distributions, on top of the perturbative component obtained via the resummation procedure. In ref. [72] the size and the universality of these effects have been discussed in detail. In codes like ResBos or DYqT a general parametrization, in the resummation formalism, allows to account for these non-perturbative contributions, whose size is intertwined with the logarithmic accuracy of the $p_\perp^W$ resummation. In the PS framework there are simple models to generate an intrinsic parton transverse momentum, with a typical size that is related to the LL accuracy of the PS resummation. The presence of heavy flavors inside the proton has an impact on the $p_\perp^W$ distributions, because of the different spectrum, with respect to the light quarks, induced by the heavy quarks PDFs.

The Cdf and DØ experiments based their description of the lepton-pair transverse momentum distribution on the code ResBos, which has NNLL-QCD accuracy in the $p_\perp^W$ resummation and a partial inclusion of the full set of NNLO-QCD corrections; for a fixed choice of the PDF set, factorization and renormalization scales, they estimated the impact on M_W of the $p_\perp^W$ modeling by varying the coefficients of the non-perturbative functions present in the resummed cross section; Cdf found this effect to be of 5 MeV (according to table XIV of ref. [1]) while DØ found it to range between 2 and 5 MeV (according to table 6 of ref. [2]), depending on the observable.

A global constraint on all these different sources of uncertainty comes from the study of the lepton-pair transverse-momentum distribution in the case of Neutral Current (NC) DY, where the gauge boson kinematics can be fully reconstructed. A detailed study of these uncertainties is beyond the scope of this paper.

2.2.2 EW and QED uncertainties: the Tevatron approach

Both Tevatron experiments, Cdf and DØ, use the ResBos generator for the treatment of QCD radiation and simulate the QED corrections to W/Z decay with Photos. As described in refs. [73–75], the EW uncertainty is derived by performing cross-checks of the Photos predictions with those of Horace-3.1 in Cdf and with those of WZgrad in DØ. The basic idea of the procedure described in those papers is that an estimate of the EW systematics can be derived by comparing independent tools which are rather different in their theoretical contents. A detailed example of this procedure can be found in ref. [76]. Actually, Photos is a process-independent tool [42, 43, 77] used at the Tevatron (as well as at the LHC) to simulate multiple photon final-state radiation (FSR) in the LL approximation, with weights to correct to the QED matrix element calculation [44]. Indeed, FSR is the largely dominant contribution to the EW corrections to W/Z production in the resonance region, as shown in many calculations and phenomenological studies [25–27, 31, 32, 34, 35]. However, pure weak corrections are neglected in Photos. On the other hand, the published versions of the WZgrad codes contain the full NLO EW corrections, without including contributions of photon radiation beyond $\mathcal{O}(\alpha)$, while Horace-3.1 is based on the matching of exact $\mathcal{O}(\alpha)$ EW corrections with multiple photon emission. Consequently, according to the experimental strategy used by both the Tevatron collaborations, the main component of uncertainty in the modeling of EW/QED processes comes from the missing inclusion of NLO EW corrections.

The present Tevatron estimate of the EW uncertainty can not be considered, strictly speaking, an evaluation of the actual theoretical uncertainty but rather an assessment of the theoretical (or physical) precision of the main tool, *i.e.* PHOTOS, used in the experimental analysis. Indeed, a more reliable estimate of the theoretical uncertainty should be associated, by definition, to the best available calculations, as induced by the most important missing higher–order contributions. From this point of view, a reassessment of the current status of EW predictions and associated QCD-EW theory results, for DY processes, provides a robust framework to put the Tevatron error estimate on firmer theoretical grounds and cross-check it according to an independent procedure. Furthermore, our results can provide a guideline for an assessment of the theoretical uncertainties in the M_W measurement at the LHC.

2.2.3 Mixed QCD-EW corrections

At NNLO accuracy level, there are three groups of perturbative terms: the $\mathcal{O}(\alpha_s^2)$, the $\mathcal{O}(\alpha^2)$ and the $\mathcal{O}(\alpha\alpha_s)$ contributions. The $\mathcal{O}(\alpha_s^2)$ terms are completely known, as already discussed in section 2.1. Among the $\mathcal{O}(\alpha^2)$ terms, the discussion of the full two-loop amplitudes renormalization has been presented in refs. [78–81]; besides the latter, two-photon and lepton-pair virtual and real emission, discussed in section 3.2, are known and yield a contribution which is classified as dominant in an expansion in powers of the enhancement factor $L_{\rm QED}$. The mixed $\mathcal{O}(\alpha\alpha_s)$ contributions are a potential source of relevant theoretical uncertainty and, as a consequence, they deserve particular attention. For this reason, recent activities of different groups focused on the calculation of partial contributions of the full $\mathcal{O}(\alpha\alpha_s)$ perturbative corrections to the charged DY cross section and distributions. In refs.[82, 83] the $\mathcal{O}(\alpha\alpha_s)$ corrections to the decays of Z and W bosons were presented, whereas the mixed two-loop corrections to the Z boson production form factors have been computed in ref.[84]. Mixed QCD-QED virtual correction to lepton-pair production have been presented in [85], while the full set of Master Integrals relevant for the evaluation of the complete set of QCD-EW virtual corrections has been presented in ref.[86]. The double-real contribution to the total cross section for the on-shell single gauge boson production has been presented in ref.[87], while the subtraction of initial state collinear singularities can now be accomplished at $\mathcal{O}(\alpha\alpha_s)$ with the Altarelli-Parisi splitting functions presented in ref.[88]. Additional building blocks are the calculation of the complete NLO EW corrections to $V+$ jet production, including the vector boson decay into leptons [89, 90] and the calculation of NLO QCD corrections to $V+\gamma$ [91–93].

A systematic approach to the calculation of mixed QCD and EW corrections to DY processes has been presented recently in refs. [94–97], adopting the pole approximation, which has been proven to give reliable predictions at NLO accuracy for observables dominated by a resonant W boson [24, 27]. In this approximation the corrections split naturally into factorizable corrections to W production and decay (for which the results of on-shell production and decay can be used as building blocks) and non-factorizable corrections, which consist of virtual and real soft photons ($E_\gamma \ll \Gamma_W$) connecting the W production and decay stages as well as soft photons connecting a final state quark and the lepton. The latter ones, which are not enhanced by collinear logarithms, have been calculated in

ref. [94] and found to be numerically well below the 0.1% level for the lepton-pair transverse mass as well as for the lepton transverse momentum distribution. Additionally, these corrections are flat over the entire range of the considered observables. As a consequence the non-factorizable $\mathcal{O}(\alpha\alpha_s)$ contributions have a negligible impact on the M_W determination.

The factorizable $\mathcal{O}(\alpha\alpha_s)$ corrections comprise three main classes of contributions: "initial-initial", consisting of virtual and real parton and photon insertions in the initial state; "final-final", consisting of virtual contributions from two-loop counterterms; "initial-final", consisting of NLO QCD (virtual and real) corrections to the W production process and NLO EW (virtual and real) corrections to the W decay. The latter class, *i.e.* "initial-final", is expected to give the bulk of the total factorizable corrections. In fact to this class contribute initial state logarithms of QCD origin and final state collinear logarithms of QED origin. In refs. [94, 96, 97] the calculation of the "initial-final" $\mathcal{O}(\alpha\alpha_s)$ [*] corrections is detailed in all its components: double-virtual, real×virtual and double-real contributions. Only the latter are not completely factorized into a product of NLO QCD and EW corrections. The factorized "initial-final" corrections, computed in pole approximation in a full calculation, are compared with the ansatz of complete factorization of the NLO corrections $\delta'_{\alpha_s}\delta_\alpha$ [†], computed separately and then multiplied, for the lepton-pair transverse mass and lepton transverse momentum distributions. In the case of the transverse mass a good level of agreement between the complete calculation and the factorized ansatz is found. Instead, in the case of the lepton transverse momentum distribution the factorized ansatz differs from the full result obtained in pole approximation.

In section 3.3 we describe the factorized ansatz for the combination of QCD and EW effects on which the formulation of POWHEG is based; in section 6.4.1 we compare the POWHEG results with those of refs. [94–97] concerning the impact on the M_W determination of factorizable $\mathcal{O}(\alpha\alpha_s)$ corrections.

3 Theoretical tools

3.1 The HORACE-3.1 formulation

The HORACE-3.1 event generator merges the exact $\mathcal{O}(\alpha)$ corrections to the CC and NC DY processes with an all order QED-PS, with photons being radiated from all the electrically charged scattering particles. It reaches NLO-EW accuracy in the description of the observables inclusive over QED radiation and it includes the effects of the all order resummation of the final state collinear mass logarithms, with LL accuracy. The double counting between the exact matrix elements and the PS algorithm is avoided, relying on the following formula for the event generation:

$$d\sigma^{\infty} = F_{SV}\ \Pi(Q^2,\varepsilon)\sum_{n=0}^{\infty}\frac{1}{n!}\left(\prod_{i=0}^{n}F_{H,i}\right)|\mathcal{M}_{n,LL}|^2 d\Phi_n \tag{3.1}$$

[*] Also the "final-final" corrections have been calculated and shown to be numerically negligible.

[†] δ_α is the relative NLO EW correction w.r.t. the LO cross section and δ'_{α_s} is the relative NLO QCD correction w.r.t. to the LO contribution calculated with NLO parton distribution functions.

The basic structure in equation (3.1) for the fully differential cross section is the sum over all photon multiplicities that accompany the hard scattering process (in this notation $n = 0$). The emission of n photons is described by LL-accurate matrix elements $\mathcal{M}_{n,LL}$, with phase space $d\Phi_n$; the unitarity of the process is guaranteed by the Sudakov form factor $\Pi(Q^2, \varepsilon)$, with Q^2 the hard scale of the process and ε the photon-energy detection threshold. The effect of the exact $\mathcal{O}(\alpha)$ matrix elements is given by the correction factors F_{SV} and $F_{H,i}$; the latter are by construction IR-finite, since the full IR divergent structure is already present in the all orders LL formulation. The virtual corrections are given by the overall factor $F_{SV} = 1 + \delta_{SV}$, where δ_{SV} is a term of $\mathcal{O}(\alpha)$, dependent on the LO kinematical invariants; it includes the effect of the renormalization scheme-dependent terms, of all the virtual diagrams and in particular of the loops where weak massive bosons are exchanged, whose effect becomes sizeable at large partonic center-of-mass energies. The one-photon real matrix element corrections $F_{H,i} = 1+\delta_{H,i}$, where $\delta_{H,i}$ is a term of $\mathcal{O}(\alpha)$, are applied to each photon emission labelled by the index i and are evaluated with an effective single-photon kinematics configuration. The presence of the correction factors $F_{H,i}$ for all emissions does not spoil the LL accuracy of the resummation via PS, which is important in the description of soft and/or collinear QED radiation. The exact NLO-EW accuracy is preserved as it can be checked by expanding equation (3.1) up to $\mathcal{O}(\alpha)$. There are several terms of $\mathcal{O}(\alpha^2)$ and higher which are introduced because of the factorized structure of equation (3.1); their effect is beyond the accuracy of the calculation; we recognize those generated by the product of F_{SV} with all photon multiplicities and those due to the product of one $F_{H,i}$ factor with the description of further real photon emissions.

The public version of the HORACE-3.1 code allows to generate events in various approximations that account for the effect of different gauge invariant subsets of corrections: 1) one FSR photon in QED-LL approximation; 2) multiple FSR photon radiation in QED-LL approximation; 3) exact $\mathcal{O}(\alpha)$ NLO-EW corrections; 4) exact $\mathcal{O}(\alpha)$ NLO-EW corrections matched with multiple-photon radiation from all the charged legs of the process in QED-LL approximation. The cases 1) and 2) are obtained from eq. (3.1) by setting $F_{SV} = F_{H,i} = 1$ and by a consistent description only of final state radiation[‡]. We stress that the outcome of points 1), 2) and 4) depends on the details of the HORACE-3.1 implementation of multiple photon radiation and on the matching scheme adopted to merge fixed- and all-order results. Alternative results, that share the same nominal accuracy and differ by subleading higher-order terms, can be found in PHOTOS[44] for approximations 1) and 2) or in the EW part of POWHEG-V2[64] for approximation 4). A new subset of $\mathcal{O}(\alpha^2)$ corrections, namely those due to the emission of an additional lepton pair, are now implemented in HORACE-3.1 and will be described in section 3.2. The effects induced by a change of the renormalization scheme, which is an option present in the code, will be discussed instead in section 4.1.

[‡]We remind that for the CC DY process the treatment of FS QED–like corrections poses problems of gauge invariance. When referring to FS radiation, it is understood that the contribution of both lepton and internal W photon emission is consistently included in the calculations without violating gauge invariance. For the NC DY process this difficulty is absent, FS QED contributions being a gauge–invariant subset of the full EW correction.

3.2 Lepton-pair corrections in HORACE-3.1

In the theoretical tools used at the Tevatron and, in particular, in the publicly available version of the HORACE-3.1 generator, the contribution due to the emission of photons converting into lepton pairs is not accounted for. The corresponding correction, of the order $\alpha^2 L^2$, is *a priori* at the same level as the two–photon contribution considered in the experimental analysis. Therefore, it is important to understand how the M_W measurement is influenced by this effect. To this end we have introduced the possibility of accounting for the emission of extra lepton pairs in the HORACE-3.1 PS mode describing QED FSR. The procedure is based on the Structure Function (SF) approach [98–100] and closely follows the recipe described in ref. [101], used in the 1990s to calculate initial-state pair corrections to the Z line shape parameters [102]. In its standard collinear formulation, the SF method provides the probability of finding a fermion inside a parent fermion whose energy has been reduced by a factor x because of the emission, at a given energy scale Q, of (strictly collinear) QED "partons". The energy loss is due to photon radiation and/or the emission of an additional light–fermion pair. Accordingly, the SF can be organized into a Non–Singlet (NS) $D^{NS}(x,Q^2)$ contribution (if the emitting fermion arrives at an annihilation or detection point without passing through a photon line) and a Singlet (S) $D^{S}(x,Q^2)$ contribution (if the fermion transforms into a fermion passing through a photon line).

In the SF language, the probability of radiating a fermion pair can be expressed using a running electromagnetic coupling constant, whose value is related to the number of emitted flavors, *i.e.* [101]

$$\alpha(s) = \begin{cases} \alpha/\left(1-\frac{\alpha}{3\pi}\ln\frac{s}{m_e^2}\right) & \text{electrons only} \\ \alpha/\left(1-\frac{\alpha}{3\pi}\ln\frac{s}{m_e^2}-\theta(s-m_\mu^2)\frac{\alpha}{3\pi}\ln\frac{s}{m_\mu^2}\right) & \text{electrons + muons} \end{cases} \tag{3.2}$$

The explicit analytical expressions of the QED SF are usually given in powers of the expansion parameter $\beta_f \equiv 2\frac{\alpha}{\pi}\log\left(\frac{s}{m_f^2}\right)$, where f indicates the flavor of the radiating particle (not to be confused with the flavor of the additional emitted pair) and s the squared energy scale of the process under consideration. When using a running coupling constant, the definition of $\beta_f(s)$ is

$$\beta_f(s) = \int_{m_f^2}^{s} \frac{ds'}{s'}\,\frac{2\alpha(s')}{\pi} \tag{3.3}$$

For the NS contribution, the effect of a light fermion pair emission from an emitting particle of flavor f can be simply taken into account with the replacement $\beta_f \to \beta_f(s)$ in the analytical expression of the SF $D^{NS}(x,Q^2)$ [100, 101].

Therefore, for electrons or muons coming from the W decay and emitting electron and

muon pairs, the formulae of interest, as obtained from eq. (3.3), are

$$\beta_f(s) = \begin{cases} 2\frac{\alpha}{\pi}\log\frac{s}{m_f^2} & f=e,\mu \quad \text{no pair emission} \\ 6\left(\log\left(1-\frac{\alpha}{3\pi}\log\frac{m_f^2}{m_e^2}\right)-\log\left(1-\frac{\alpha}{3\pi}\log\frac{s}{m_e^2}\right)\right) & f=e,\mu \quad e^+e^- \text{emission} \\ -3\log\left(\left(1-\frac{\alpha}{3\pi}\log\frac{s}{m_e^2}\right)^2-\left(\frac{\alpha}{3\pi}\right)^2\log^2\left(\frac{s}{m_\mu^2}\right)\right) & f=e \quad e^+e^- \text{ and } \mu^+\mu^- \text{emission} \\ 3\log\frac{1-\frac{\alpha}{3\pi}\log\frac{s}{m_e^2}+\frac{\alpha}{3\pi}\log\frac{s}{m_\mu^2}}{1-\frac{\alpha}{3\pi}\log\frac{s}{m_e^2}-\frac{\alpha}{3\pi}\log\frac{s}{m_\mu^2}} & f=\mu \quad e^+e^- \text{ and } \mu^+\mu^- \text{emission} \end{cases} \tag{3.4}$$

In the PS algorithm implemented in HORACE-3.1 these contributions have been included by means of an appropriate modification of the Sudakov form factor and the calculation of the fractions of the emitted electron and muon pairs, as detailed in appendix B.

In addition to the NS contribution, one must also include the singlet contribution to the QED SF, as given *e.g.* in ref. [101]. However, we checked that the numerical impact of $D^S(x,Q^2)$ on the relevant observables is negligible at the precision level of interest here, the singlet SF being numerically suppressed with respect to $D^{NS}(x,Q^2)$ for any x value and vanishing in the most relevant phenomenological region, *i.e.* in the infrared limit $x \to 1$.

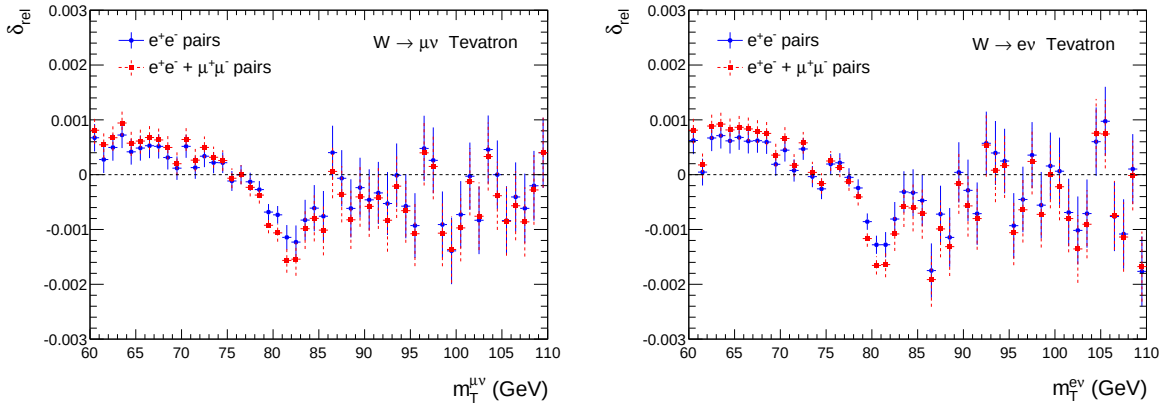

Figure 1. Relative effect due to lepton-pair corrections on the W transverse mass distribution, for $W \to \mu\nu$ (left plot) and $W \to e\nu$ (right plot) decays at the Tevatron ($\sqrt{s} = 1.96$ TeV). The plots show the relative difference between the HORACE-3.1 predictions for multiple FSR with and without pair emission.

The numerical impact on the W transverse mass distribution due to lepton-pair emission in $W \to e\nu$ and $W \to \mu\nu$ decays at the Tevatron energy ($\sqrt{s} = 1.96$ TeV) is shown in figure 1. The relative contribution shown in figure 1 is computed in terms of HORACE-3.1 predictions for the combined multiple photon and pair radiation normalized to the results for multiple photon radiation only. As can be seen, the correction is largely dominated by the contribution of the lightest radiated particles, *i.e.* by electron pair emission, which is a direct consequence of eq. (3.4). Around the Jacobian peak, the pair correction amounts to about $0.1 - 0.2$ % for both decay channels and modifies the shape of the transverse mass distribution, similarly to the effect introduced by photon emission [25, 27, 34, 103].

3.3 POWHEG with QCD and EW corrections

The implementation of the CC DY process in POWHEG is documented in ref. [104], at NLO QCD accuracy. The extension to include both NLO QCD and NLO EW corrections for this process in POWHEG is documented in refs. [64, 65] [§]. In this implementation, the overall cross section has NLO (QCD+EW) accuracy, and the real radiation can be of QCD as well as QED origin. According to the POWHEG method, the cross section for a given process is written as:

$$d\sigma = \sum_{f_b} \bar{B}^{f_b}(\mathbf{\Phi}_n)\, d\mathbf{\Phi}_n \Bigg\{ \Delta^{f_b}(\mathbf{\Phi}_n, p_T^{min}) + \sum_{\alpha_r \in \{\alpha_r | f_b\}} \frac{\left[d\Phi_{rad}\, \theta(k_T - p_T^{min})\, \Delta^{f_b}(\mathbf{\Phi}_n, k_T)\, R(\mathbf{\Phi}_{n+1}) \right]_{\alpha_r}^{\bar{\mathbf{\Phi}}_n^{\alpha_r} = \mathbf{\Phi}_n}}{B^{f_b}(\mathbf{\Phi}_n)} \Bigg\} . \quad (3.5)$$

The function $\bar{B}^{f_b}$ gives the NLO (QCD+EW) inclusive cross section, and the term between curly brackets controls the hardest emission (for more details on the notation, see ref. [105]). The inclusion of NLO EW corrections, with respect to the version including only QCD corrections, amounts to a modification of $\bar{B}^{f_b}$ in order to include the virtual EW and real QED contributions, and the addition of subtraction counterterms and collinear remnants corresponding to the new singular regions, i.e. the ones associated with the emission of a soft/collinear photon by a hard scattering quark or a soft photon by the final state lepton. It is worth reminding that in refs. [64, 65] the final state leptons have been treated with full mass dependence, in order to deal in a proper way with all event selections of experimental interest: bare as well as dressed leptons. In this formulation, the photons collinear to leptons give rise to logarithmic but not singular terms and they do not need subtraction. The Sudakov form factor $\Delta^{f_b}(\mathbf{\Phi}_n, k_T)$ is the product of individual factors defined for each singular region, so it has been modified as well in order to take care of the additional singular regions.

The POWHEG algorithm generates the hardest emission of the event by probing in sequence all the singular regions described by the various Sudakov form factors and eventually choosing the radiated parton with largest transverse momentum. In this sense, the generation of a photon, either from the initial state or from the final state by POWHEG is in competition with the generation of a parton. Notice that expanding eq. (3.5), on top of $\mathcal{O}(\alpha)$ and $\mathcal{O}(\alpha_s)$ corrections for the cross section, also higher order terms, in particular of $\mathcal{O}(\alpha_s^2)$ and of $\mathcal{O}(\alpha\alpha_s)$, appear and affect the description of differential distributions. This is described in more detail in section 4.2.

The matching of the generated events with the PS, reaching the so called NLOPS accuracy, is naturally done using a p_T ordered PS: the emissions start down from the scale set by POWHEG (p_T of the hardest radiated particle). This is automatically implemented for the QCD PS when using PYTHIA. Here there is a subtlety: the default definition of hardness of the PS emissions is usually kinematically different from the way the variable

[§] An independent implementation of EW corrections to the CC DY process is presented in ref. [63].

"scalup" is calculated in POWHEG at the level of the Les Houches event file generation (the different definitions agree in the limit of collinear radiation). In our simulations we use the version V2 of the POWHEG-BOX, abbreviated in the following POWHEG-V2, where we provide the interface to PYTHIA8 and PHOTOS++. In this interface we allow for QCD and QED radiation of partons or photons up to the kinematical limit and then we veto the radiation when one PS radiated parton or photon does not respect the limit imposed by "scalup", calculated according to the POWHEG definition. The same strategy is adopted for the QED radiation from the resonance, either if it is treated with PYTHIA8 (where, by default, the starting scale is the resonance mass) or if it is treated by PHOTOS++, which does not generate p_T ordered radiation.

In order to perform our studies, we added a switch to turn on and off the NLO EW corrections directly from the input file, thus allowing consistent and tuned estimates of the EW effects. We also included an interface to PHOTOS++, which takes as input the POWHEG event file; and then writes a second LHE event file containing also the photons generated by PHOTOS++, as a preliminary step before the ISR radiation described by the Parton Shower. This second file is written in standard `.lhe` format and can be read by any other PS Monte Carlo for additional QCD/QED radiation from partons. When using this interface to PHOTOS++, the QED radiation from W and Z resonances should be switched off in the PS Monte Carlo, to avoid double counting.

An important remark on the lepton event selection is in order. By using fully massive kinematics for leptons, the generator can handle, in principle, any event selection, including, in particular, bare leptons, i.e. the lepton momentum is never recombined with any photon. However, at the generation stage, the separation between radiative events, with resolved photon radiation, and elastic events, with unresolved photon radiation, is done through the relative transverse momentum between lepton and photon. This means that, in principle, the lepton can never be considered bare (for this it would be necessary to set the resolution parameter `kt2minqed`[¶] to zero, which produces an infrared divergence). In practice, since the peak of the distribution of the relative momentum between lepton and photon is of the order of m_ℓ, the lepton can be considered as a bare lepton if the condition `kt2minqed` $\ll m_\ell^2$ is fulfilled. While for muons this is the case for the default value `kt2minqed`$= 10^{-6}$ GeV^2, for electrons it would be required to set the scale to much lower values. Since at the LHC bare leptons are experimentally well defined only for muons, the results obtained in this study with POWHEG are presented accordingly only for bare muons and dressed electrons. We observe that the default value of `kt2minqed` is consistent with the definition of dressed electrons.

3.3.1 POWHEG-V2 `two-rad` improved version for DY processes

The above brief description of the POWHEG code for the CC DY process applies to the library W_EW-BMNNP svn version 3348 (the same applies to Z_EW-BMNNPV svn version 3347 for the NC DY process). In the treatment of both QCD and ISR/FSR QED

[¶] The parameter `kt2minqed` sets in POWHEG-V2 the lowest possible value of the transverse momentum of an emitted real photon.

radiations there is a potential problem at the level of event generation, which can become phenomenologically important for some exclusive observables.

In fact, the largest transverse momentum of a coloured parton or photon, extracted by means of the Sudakov form factor, sets the maximum scale of the (QCD and QED) PS radiation. On average, the scale of QCD radiation, obtained by the inversion of the ISR Sudakov form factor, is larger than the one of QED FSR, obtained by the inversion of the QED FSR Sudakov form factor. As a consequence, the POWHEG first radiation is typically a QCD parton which sets the scale for both QCD and QED PSs. This behaviour entails a double counting between QED radiation from matrix element and PS, which can become severe for observables particularly sensitive to final state QED radiation, as is the case under study in the present work (quantitative estimates of the impact on M_W of the effect will be given in section. 6.4.4). Additionally, also spurious $\mathcal{O}(\alpha\alpha_s)$ corrections can be introduced.

A way out of this problem is provided by the general treatment of the NLOPS matching of ref. [12] in the presence of radiation from final state resonances. According to this approach, the competition between QCD and QED radiation is present only in the initial state. The QED radiation from the W resonance is treated separately and, in particular, the hardest photon scale, obtained through the inversion of the FSR QED Sudakov form factor, is kept as input to the QED PS from the resonance. Moreover, the events generated by the current release of POWHEG-BOX-V2 (W_EW-BMNNP svn version newer than 3348 and Z_EW-BMNNPV svn version newer than 3347) can contain up to two radiated particles (one ISR parton/photon and one FSR photon) and the information about the two ISR and FSR scales. For this reason the matching with the QCD and QED PSs has been modified with respect to the original version described in section 3.3. We have modified the POWHEG-V2/W_EW-BMNNP code according to the approach of ref. [12] [‖] [**]; we dub `two-rad` this improved version.

In figure 2 we show the lepton-neutrino invariant mass, which is the most sensitive observable to different treatments of QED radiation, since the relative QED correction can become very large for this distribution, up to 60% of the lowest order prediction, as it can be seen from the inset of the figure. The blue dots represent the relative difference between the predictions of POWHEG-V2 with NLO QCD+EW corrections interfaced to PYTHIA+PHOTOS and the predictions of POWHEG-V2 with only NLO QCD corrections interfaced to PYTHIA+PHOTOS. As it can be seen, the differences start around the W mass peak and reach the maximum ($\sim$ 2%) at $M(\mu^+\nu) \simeq 70$ GeV. The red dots show the corresponding difference for the `two-rad` upgraded version of POWHEG-V2. With respect to the predictions of POWHEG-V2 with only NLO QCD corrections interfaced to

[‖] A general POWHEG-BOX-RES version, able to treat in an automatic way arbitrary processes with resonances, is under development. It has already been applied to the simulation of t-channel single-top production [12] and $pp \to \ell^+\nu_\ell\ell^-\bar{\nu}_\ell b\bar{b}$ [106]. For the DY case we simply modify the V2 process libraries, since other subtleties related to the presence of resonance and additional particles in the final state do not affect the DY processes. In any case, the DY process libraries will be also available under the POWHEG-BOX-RES version.

[**]Similar considerations hold also for the Z_EW-BMNNPV package.

PYTHIA+PHOTOS, there is a moderate slope but the relative effects are well below the % level in the region around the W mass peak, where the bulk of the cross section is concentrated. The same relative difference is investigated in figure 3 for the W transverse mass (left plot) and for the lepton transverse momentum (right plot). Since the QED corrections to these two observables are smaller w.r.t. the ones for the lepton-pair invariant mass, the differences between POWHEG-V2 standard version and the `two-rad` upgraded one are much smaller. However we can note a difference reaching the 0.5% level on the transverse mass around the jacobian peak and a mild slope in the lepton transverse momentum distribution. These different shapes are at the origin of the differences of the shifts ΔM_W discussed in section 6.4.4.

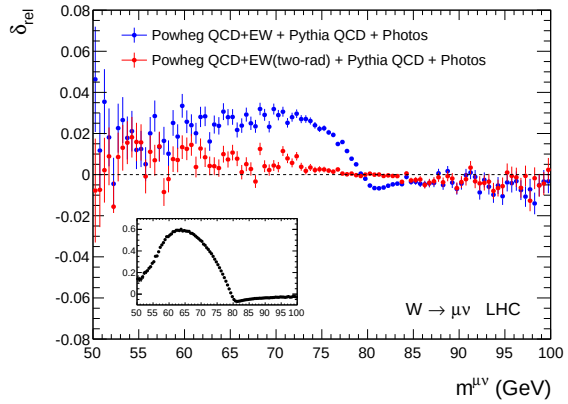

Figure 2. Relative difference, for the $\mu^+\nu$ invariant mass distribution, normalized to the prediction of POWHEG-V2 with NLO QCD corrections interfaced to the PYTHIA QCD PS, of two different implementations of EW corrections: predictions of POWHEG-V2 `two-rad` with NLO QCD+EW corrections (red dots), and of the old version of POWHEG-V2 with NLO QCD+EW corrections (blue dots). Both codes are interfaced to the PYTHIA QCD PS and to PHOTOS. For reference, the EW corrections normalized to the LO are reported in the insets.

4 Perturbative uncertainties

4.1 EW input scheme

The evaluation of the NLO-EW corrections requires a renormalization procedure to define the couplings and the masses which appear in the scattering amplitudes; the renormalized parameters are then expressed in terms of physical observables. The couplings of the gauge sector of the EW SM, namely the $SU(2)_L$ and $U(1)_Y$ gauge couplings (g, g'), the vacuum expectation value v of the Higgs doublet and the quartic coupling λ of the Higgs scalar potential, can be expressed in terms of different possible sets of measured quantities. The difference between two input choices can be regarded as a finite renormalization; as such, it yields terms of higher perturbative order, with respect to the NLO-EW accuracy of the calculation, namely terms of $\mathcal{O}(\alpha^2)$.

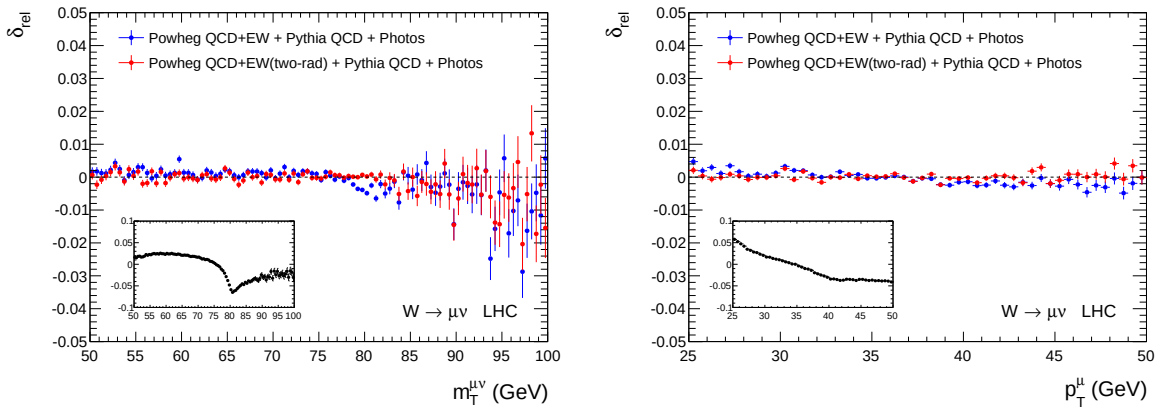

Figure 3. Same as in figure 2 for the lepton-pair transverse mass (left plot) and for the lepton transverse momentum (right plot).

The input parameter choices affect not only the overall normalization of the cross section, but also the precise shape of the differential distributions and eventually the M_W determination. The size of these effects depends on the precise formulation of the calculation, whether it is a purely fixed order analysis or whether it involves the matching of exact matrix elements with a Parton Shower.

We consider in this section three input schemes: the so called α_0 scheme and two variants of the so called G_μ scheme. The α_0 scheme is based on the use, as input parameters, of $(\alpha(0), M_W, M_Z, M_H)$, which are respectively the Thomson value of the fine structure constant and the W, Z and Higgs boson masses; the renormalization is performed in the on–shell scheme, computing the counterterms associated to the electric charge, the W and Z boson masses. As shown in the literature [27, 31], this scheme turns out to be rather unnatural for the description of the CC DY process, because it maximizes the contribution of NLO EW corrections through the fermion–loop contribution to the W self–energy. The latter can be reabsorbed in the measured value of the muon decay constant G_μ and the input parameter scheme defined in terms of the quantities (G_μ, M_W, M_Z, M_H) is known as G_μ scheme, typically used in the literature for the calculation of the radiative corrections to the CC DY process. However, the α_0 option, in spite of its drawbacks, can not be left out *a priori*, being a fully consistent and predictive theoretical scheme.

The choice of the EW input scheme affects the computation of the observables of the CC DY process in the presence of exact $\mathcal{O}(\alpha)$ corrections. To introduce the G_μ scheme, it is worth noting that the EW tree–level amplitude is proportional to the $SU(2)$ gauge coupling g^2 rather than to α_0. Therefore it is possible to exploit the well known relation between the muon decay constant G_μ and the radiative corrections to the muon decay amplitude represented by the Δr parameter to write

$$\frac{G_\mu}{\sqrt{2}} = \frac{g^2}{8M_W^2}\,(1+\Delta r)\ . \tag{4.1}$$

For later convenience, we introduce the effective electromagnetic coupling α_μ, at tree–level

Scheme	F_{SV}	Couplings of $\lvert\mathcal{M}_{n,LL}\rvert^2$
α_0	$1+\alpha_0\frac{\sigma_{SV}-\sigma_{SV}^{LL}}{\sigma_0}$	$\alpha_0^2\alpha_0^n$
$G_\mu\ I$	$1+\alpha_0\frac{\sigma_{SV}-\sigma_{SV}^{LL}}{\sigma_0}-2\Delta r$	$(\alpha_\mu^{tree})^2\alpha_0^n$
$G_\mu\ II$	$1+\alpha_0\frac{\sigma_{SV}-\sigma_{SV}^{LL}}{\sigma_0}$	$(\alpha_\mu^{1l})^2\alpha_0^n$

Table 1. Comparison of different renormalization input schemes: structure of the F_{SV} soft+virtual correction factor and proportionality factor of the matrix element describing the emission of n real photons.

and in one–loop approximation, according to the following definitions:

$$\alpha_\mu^{tree} \equiv \frac{\sqrt{2}}{\pi} G_\mu M_W^2 \sin^2\theta_W\,, \tag{4.2}$$

$$\alpha_\mu^{1l} \equiv \frac{\sqrt{2}}{\pi} G_\mu M_W^2 \sin^2\theta_W\,(1-\Delta r)\,, \tag{4.3}$$

where $\sin^2\theta_W = 1 - M_W^2/M_Z^2$ is the squared sine of the on-shell weak mixing angle. In the G_μ scheme, the Born cross section σ_0 is proportional to $(\alpha_\mu^{tree})^2$. When performing a complete $\mathcal{O}(\alpha)$ calculation in this scheme, it is necessary to add a finite countertem $(-2\sigma_0\Delta r)$ to the virtual corrections to avoid a double counting of the Born contribution, expressed in terms of G_μ, already present in the diagrammatic results.

We write schematically the $\mathcal{O}(\alpha)$ cross section in the α_0 and G_μ schemes, making explicit the dependence on the couplings at the different perturbative orders (σ_{SV} and σ_H label the soft+virtual and the real hard emission contributions) and distinguishing two possible options for the G_μ scheme. We have in principle the three following alternatives, which differ by $\mathcal{O}(\alpha^2)$ corrections:

$$\alpha_0 \ : \quad \sigma = \alpha_0^2\sigma_0 + \alpha_0^3(\sigma_{SV}+\sigma_H)\,, \tag{4.4}$$

$$G_\mu\ I \ : \quad \sigma = (\alpha_\mu^{tree})^2\sigma_0 + (\alpha_\mu^{tree})^2\alpha_0(\sigma_{SV}+\sigma_H) - 2\Delta r(\alpha_\mu^{tree})^2\sigma_0\,, \tag{4.5}$$

$$G_\mu\ II \ : \quad \sigma = (\alpha_\mu^{1l})^2\sigma_0 + (\alpha_\mu^{1l})^2\alpha_0(\sigma_{SV}+\sigma_H)\,. \tag{4.6}$$

We introduce the idea of sharing i.e. the relative percentage of 0– and 1–photon contributions with the real-photon energy greater than a certain threshold. The 0–photon subset receives contributions from the Born cross section and from the soft+virtual $\mathcal{O}(\alpha)$ corrections; the latter contain in particular the renormalization terms. As a consequence of eqs. (4.4-4.6), we show in table 1 the expression of the correction factors F_{SV}, introduced in section 3.1. It can be seen that the correction factors F_{SV} in the α_0 and in the $G_\mu\ II$ schemes are the same, while the factor in the $G_\mu\ I$ scheme is different. Concerning the squared matrix elements $\lvert\mathcal{M}_{n,LL}\rvert^2$ according to the three options, we show in table 1 their dependence on the coupling constant; the correction factors $F_{H,i}$ of eq. (3.1) are equal in the three schemes since the same proportionality is present in the exact squared matrix elements $\lvert\mathcal{M}_n\rvert^2$. In summary, the EW input schemes described above yield a different sharing of 0– and 1–photon events, which in turn can imply a different distortion of the

distributions used to extract the W boson mass. In particular, the α_0 and the G_μ II schemes have the same sharing, despite of the different normalization.

Now we consider the matching of NLO-EW results with a QED PS, as described in eq. (3.1). It is worth noticing that the sharing of the different photon multiplicities is the same in the three schemes discussed above, as can be deduced from the facts that the $F_{H,i}$ factors are the same and F_{SV} is factorized. As a consequence, we expect that the sensitivity of the matched cross section as given by eq. (3.1) to the input scheme choice is reduced w.r.t. the pure $\mathcal{O}(\alpha)$ prediction. We stress that the F_{SV} factor is not constant with respect to the kinematical invariants, but it has a mild dependence on them and thus it can still modify the shape of the distributions.

While eq. (3.1) describes the structure of a purely EW event generator, it is interesting to consider how the input parameter choices affect the predictions of POWHEG, whose formulation is shown in eq. (3.5), where QCD and EW corrections are mixed. The EW virtual corrections and all the terms associated with the renormalization are included in the factor $\bar{B}(\mathbf{\Phi}_n)$. Similarly to the purely EW case, this factor has a mild dependence on the event kinematics and it rescales in the same way all the real parton multiplicities.

4.2 Mixed $\mathcal{O}(\alpha\alpha_s)$ corrections

Due to the factorization properties of the IR soft/collinear singularities of QCD and QED origin, the available generators, used to extract M_W by fitting the experimental data, effectively include the leading structures of the factorized mixed QCD-EW corrections. It is therefore important to investigate the role of the $\mathcal{O}(\alpha\alpha_s)$ terms included in these generators and to attempt an estimate of the impact on M_W of the residual $\mathcal{O}(\alpha\alpha_s)$ corrections which are not available in the codes.

The distributions predicted by the code adopted in the Tevatron analysis, *i.e.* RESBOS+ PHOTOS, include the effects, in a factorized form, of initial state QCD corrections and of final state QED corrections. In the present study we consider a similar combination, which is obtained in POWHEG-V2 code with NLO (QCD+EW) corrections, by switching off NLO EW corrections and by including QED-LL final-state corrections to all orders by means of PHOTOS or PYTHIA8 (for the latter code we dub the corresponding routines PYTHIA-QED, to distinguish them from the QCD ISR PS); this combination includes terms of order

$$\alpha_s\alpha\left(c_2 L_{\rm QCD}^2 + c_1 L_{\rm QCD} + c_0\right)\left(c_{11} L_{\rm QED} l_{\rm QED} + c_{10} L_{\rm QED} + c_{01} l_{\rm QED}\right)\,, \tag{4.7}$$

where $L_{\rm QCD}$ stands for the logarithm of the scale of the process Q^2 over the square of the dimensionful observable under study, $L_{\rm QED} = \log\left(Q^2/m_l^2\right)$ (m_l being the mass of the final state charged lepton) and l is the log of soft infrared origin, effectively generated by the applied cuts.

If, on the other hand, we consider the code POWHEG-V2 with the NLO EW corrections turned on and QED-LL final-state corrections accounted for to all orders by means of PHOTOS (or PYTHIA-QED), the included $\mathcal{O}(\alpha\alpha_s)$ terms have the form

$$\alpha_s\alpha\left(c_2 L_{\rm QCD}^2 + c_1 L_{\rm QCD} + c_0\right)\left(c_{11} L_{\rm QED} l_{\rm QED} + c_{10} L_{\rm QED} + c_{01} l_{\rm QED} + c_{00}\right)\,, \tag{4.8}$$

With respect to eq. (4.7), eq. (4.8) contains in addition the term

$$\alpha_s \alpha \, c_{00} \left(c_2 L_{\rm QCD}^2 + c_1 L_{\rm QCD} + c_0 \right) .$$

This term is available in POWHEG-V2 as a consequence of the factorized structure of eq. (3.5) and reproduces correctly a subset of $\mathcal{O}(\alpha\alpha_s)$ in the limit of collinear QCD radiation. Its inclusion represents a possible improvement of the simulation tools used in the M_W studies, although the $\mathcal{O}(\alpha\alpha_s)$ accuracy can not be claimed because the complete set of the exact matrix elements with this perturbative accuracy is not available. On the other hand, this term is missing in the Tevatron analysis and should thus be treated as a source of theoretical uncertainty affecting the Tevatron M_W determination; we investigate this point in the following sections.

5 Impact of radiative corrections on the kinematical distributions

In order to set the stage of the discussion, we present in figure 4 the impact of exact fixed-order corrections to the lepton-pair transverse mass distribution, with muons in the final state, at the LHC with $\sqrt{s} = 14$ TeV, in the case of W^+ production. We consider NLO QCD, NLO EW effects and the sum of the two sets of corrections and we show their relative impact normalized to the LO prediction. We observe the negative impact of EW corrections at the jacobian peak of the distribution and the monotonic increase due to QCD effects. When summing NLO QCD+EW corrections, we obtain a partial cancellation of the radiative effect at the jacobian peak.

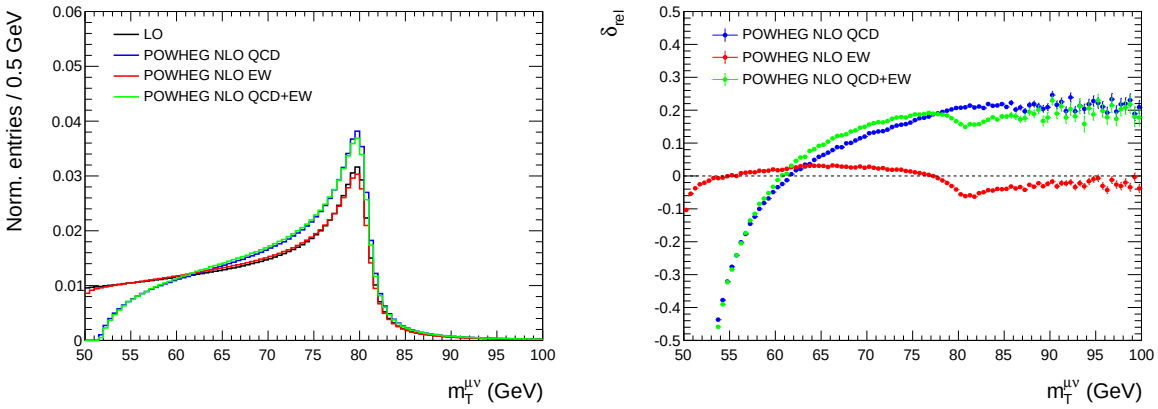

Figure 4. Fixed-order predictions for the transverse mass distribution, in the case of W^+ production with muons in the final state at LHC 14 TeV and acceptance cuts as in table 6. We show different perturbative approximations, including only NLO QCD, only NLO EW and the sum of the two sets of corrections. In the left plot we show the shape of the distributions and in the right plot the relative effect of the radiative corrections, normalized to the LO prediction.

In the following sections we study the impact of higher-order radiative corrections on the kinematical distributions relevant for the M_W determination. In particular we focus on: *i)* light lepton pairs corrections; *ii)* the modeling of QED radiation; *iii)* the influence

of QCD contributions and their interplay with purely QED FSR effects and *iv)* mixed $\mathcal{O}(\alpha\alpha_s)$ corrections beyond the approximation that combines QCD with purely QED FSR corrections.

5.1 Light lepton pairs radiation

In figure 5 we study the effect of two sets of corrections that start at $\mathcal{O}(\alpha^2)$: we show the contribution of additional light lepton pairs radiation in comparison with the contribution of multiple FSR beyond $\mathcal{O}(\alpha)$, both normalized to the distribution computed strictly with one FSR photon emission. The relative effects are calculated in the case of the decays $W \to \mu\nu$ and $W \to e\nu$ (where e is a bare electron) at the Tevatron. We observe that higher-order FSR yields at the jacobian peak an increase of the transverse mass distribution, ranging from 0.35% for muons to 1.5% for bare electrons, at variance with the $\mathcal{O}(\alpha)$ effect which is instead negative. The additional $\mathcal{O}(\alpha^2)$ contribution due to the emission of light pairs is instead negative, at the level of -0.15%, to a large extent independent of the radiating lepton. As detailed in appendix B, this behavior is simply a consequence of the

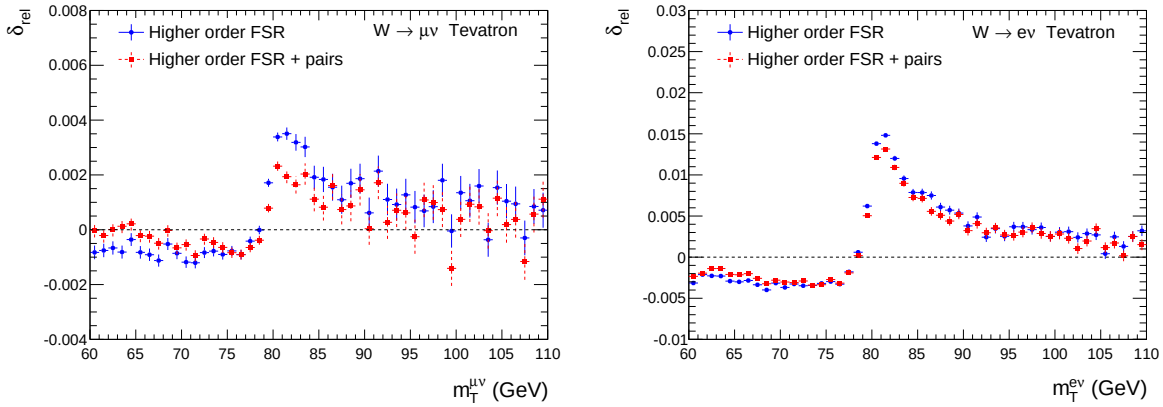

Figure 5. Relative contribution of higher-order FSR and higher-order FSR plus pair radiation normalized to one-photon emission, for W^+ decay into muons (left) and into bare electrons (right). Predictions from HORACE-3.1 at Tevatron energy, with the acceptance cuts of table 2.

dependence of the expansion parameter $\beta_f(s)$ given in eq. (3.4) on m_f, where m_f is the mass of the radiating particle of flavor f. Notice that in the case of dressed electrons, for which accompanying photons are recombined with the electrons within a given angular resolution, the contribution of FSR will diminish while the correction due to undetected lepton-pair radiation will be left unchanged. Indeed, lepton pairs, at variance with respect to photons, can not be recombined with the emitting particle, because of physical and experimental reasons.

5.2 QED FSR modeling

The description of multiple QED FSR can be achieved with different tools, like HORACE, PHOTOS or PYTHIA-QED. The M_W determination is very sensitive to the details of QED

FSR description, so that a comparison of the predictions of these three tools and the evaluation of the corresponding impact on M_W are in order. We analyze the predictions

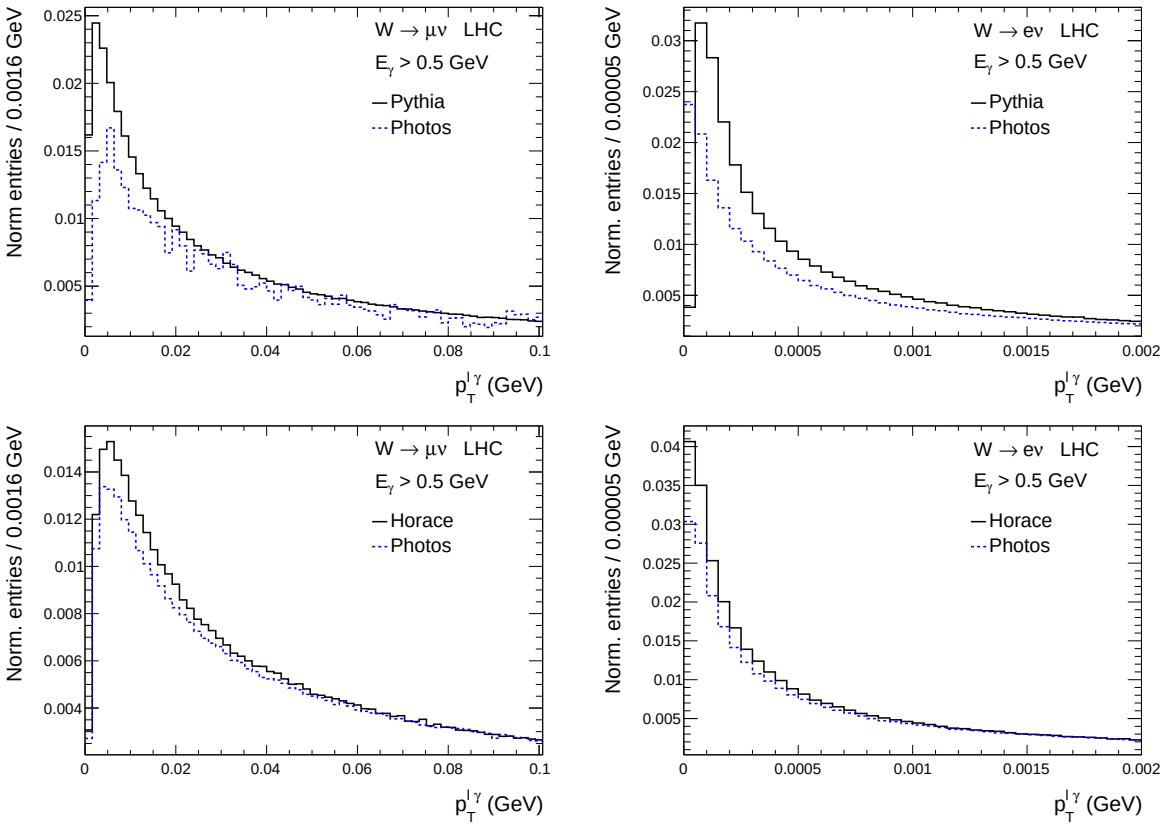

Figure 6. Shape of the distribution of the relative lepton-photon transverse momentum $p_T^{\ell\gamma}$ for the decays $W^+ \to \mu^+\nu$ (left plots) and $W^+ \to e^+\nu$ (right plots) at the LHC 14 TeV, with acceptance cuts as in table 11. In the upper plots we show the comparison of the results obtained interfacing POWHEG-V2 NLO QCD results with PYTHIA-QED and PHOTOS. In the lower plots we show the comparison of the results obtained with HORACE including QED FSR effects and those obtained interfacing HORACE LO with PHOTOS, in both cases without QCD corrections.

obtained with the three codes for the energy and angular distributions of the emitted radiation in $W \to \mu\nu$ and $W \to e\nu$ decays. We find that the predictions for the photon energy spectrum are in good agreement, whereas the angular distributions show some discrepancies.

For example, figure 6 shows the comparison of the PHOTOS, PYTHIA and HORACE predictions for the relative lepton-photon transverse momentum $p_T^{\ell\gamma}$, $\ell = \mu, e$, distributions at the LHC. We impose $E_\gamma^{\rm min} = 0.5$ GeV and we consider the events with strictly only one-photon in the final state. In the upper plots of figure 6, we focus on PHOTOS and PYTHIA-QED, which provide for this observable different predictions, with a dependence of the size of the discrepancy on the flavor of the final state bare lepton. This discrepancy disappears in the case of dressed electrons. On the other hand, as it is shown in the lower

plots of figure 6, PHOTOS and HORACE results are in much closer agreement.

The observed discrepancy can be ascribed to the theoretical model implemented in PYTHIA-QED, which simulates the angular degree of freedom of QED radiation according to the distribution dp_T/p_T, $p_T \equiv p_T^{\ell\gamma}$. On the contrary, PHOTOS and HORACE describe the angular variable using a similar model, dictated by the eikonal approximation $d\sigma/d\cos\theta \propto 1/(1-\beta\cos\theta)$, where $\cos\theta \equiv \cos\theta_{\ell\gamma}$ and β is the lepton velocity. All the three codes have LL accuracy with respect to $L_{\rm QED}$, but differ at the level of subleading terms, with different approximations of the exact matrix element for one photon emission. The different formulation allows to explain the flavor dependence of the discrepancy, with an enhancement in the case of bare electrons where $L_{\rm QED}$ has a larger value. In the case of dressed electrons, the recombination procedure integrates over the phase-space region where the discrepancy stems from, letting the latter vanish.

5.3 QCD corrections and QCD-QED interplay

Fixed- and all-orders QCD corrections have a fundamental role in the description of the observables relevant for the M_W determination. NLO QCD corrections yield a large positive increase of $\mathcal{O}(20\%)$ of the cross section and QCD multiple parton ISR is crucial for a realistic prediction of the shape of kinematical distributions. The lepton transverse momentum receives large QCD corrections, because of the presence of a logarithmic enhancement factor associated to the initial state collinear singularities; the latter require the resummation to all orders of this class of corrections and yield a sizeable effect on this observable. The lepton-pair transverse mass distribution instead is mildly affected by perturbative QCD contributions, because of a more systematic cancellation of these large logarithmic corrections.

The combination of two sets of corrections like QCD ISR and QED FSR, which separately induce large changes of the distributions, may also yield important effects at the level of mixed QCD-QED terms, which are present in simulation tools based on a factorized ansatz for the inclusion of QCD and QED terms. We show in the upper plots of figure 7 the lepton-pair transverse mass (left plot) and the lepton transverse momentum (right plot) distributions in different perturbative approximations: at LO (black), at LO convoluted with a QED PS (blue), at NLO QCD matched with a QCD PS (green) and finally at NLO QCD matched with a QCD PS and convoluted with a tool describing QED FSR to all orders (red). We dub the last approximation $\text{QCD}_{\text{NLOPS}}\times\text{QED}_{\text{PS}}$. In figure 7 we use PHOTOS as tool to describe QED FSR. The comparison of the first two approximations (blue *vs* black lines) shows the negative effect of QED FSR at the jacobian peak of both observables. The comparison of the first and of the third approximations (green *vs* black lines) shows the impact of QCD corrections with respect to the LO predictions: the lepton-pair transverse mass distribution is mildly modified by QCD effects, whereas the lepton transverse momentum distribution has a much broader and smeared shape compared to the LO one. The comparison of the third and of the fourth approximations (red *vs* green lines) shows the effect of the convolution with a tool for the simulation of QED FSR to all orders on top of the results obtained with the full set of available QCD corrections. In the lower plots of figure 7 we focus on the relative size of QED FSR effects, evaluated in terms of the

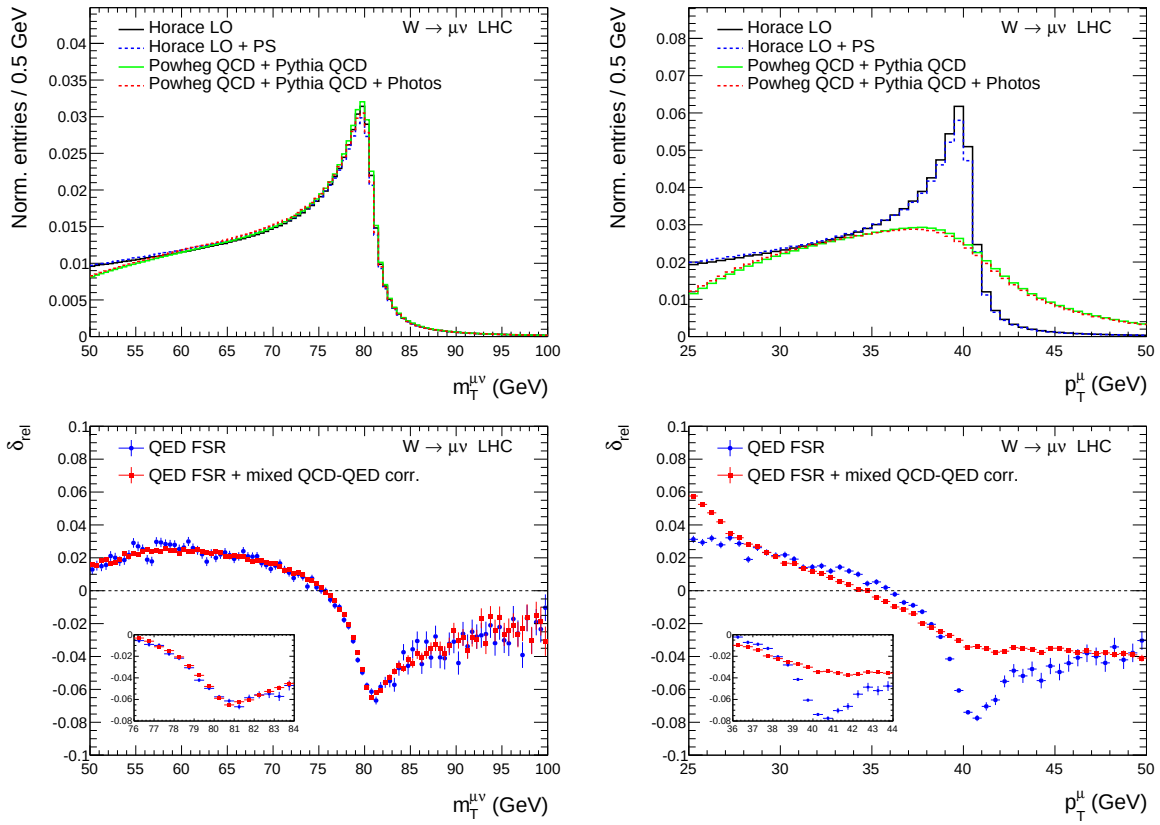

Figure 7. Upper plots: lepton-pair transverse mass (left plots) and lepton transverse momentum (right plots) distributions in different approximations: without QCD corrections (HORACE LO and HORACE with QED FSR PS) and with QCD corrections (POWHEG-V2 NLO QCD + QCD PS and POWHEG-V2 NLO QCD + QCD PS interfaced to PHOTOS) for the decay $W^+ \to \mu^+\nu$ at the LHC 14 TeV, with acceptance cuts as in table 11. Lower plots: relative contribution of QED FSR normalized to the LO predictions and of QED FSR + mixed QCD-QED corrections normalized to the POWHEG-V2 NLO QCD + QCD PS predictions.

LO predictions (blue dots); we then consider the predictions in $\text{QCD}_{\text{NLOPS}} \times \text{QED}_{\text{PS}}$ approximation and take the ratio with purely QCD corrected distributions (red dots). With this ratio we express the impact of QED FSR corrections together with the one of mixed QCD-QED terms present in a tool based on a factorized ansatz for the combination of QCD and QED terms, removing exactly the effect of pure QCD corrections. The QED FSR corrections are common to the blue and red dots and the difference between the two sets of points is induced by the mixed QCD-QED corrections. As it can be seen from figure 7, the shape and size of the QED FSR corrections to the transverse mass distribution is largely maintained after the inclusion of QCD corrections; the mixed QCD-QED contributions are moderate but not negligible, with an effect at the few per mille level. On the contrary, the lepton p_T distribution is strongly modified by mixed QCD-QED effects, which amount to some per cent and, more importantly, smear the varying shape of the

QED FSR contribution, especially around the Jacobian peak, as emphasized in previous studies [62, 64, 65].

5.4 Mixed QCD-EW corrections

As described in sections 3.3 and 3.3.1, there are two further sets of factorizable $\mathcal{O}(\alpha\alpha_s)$ corrections, beyond the ones obtained with the convolution of QED FSR effects on top of events with NLO QCD + QCD PS accuracy. The first set comes from the inclusion of the full set of EW corrections at NLO accuracy in association to QCD radiation described by a QCD PS; they are given by all the terms absent in pure QED FSR approximation of the $\mathcal{O}(\alpha)$ corrections, multiplied by the relevant QCD terms. The second set is due to the interplay of QCD effects with subleading QED terms present in different ways in the tools that model QED FSR to all orders. These two classes of factorizable QCD-EW corrections constitute a source of theoretical uncertainty, if a theoretical model like, for instance, the standard QCD POWHEG interfaced to a QED tool is adopted.

The impact of these mixed QCD-EW contributions on the lepton-pair tranverse mass and lepton transverse momentum distributions is shown in figure 8 (for W decays into muons at the LHC). In the upper plots we present the results in three approximations: *i)* the standard POWHEG-V2 with only QCD corrections, with NLO QCD + QCD PS accuracy (black line), *ii)* the same events of the previous point convoluted with PHOTOS to include QED FSR to all orders effects (blue line) and *iii)* events generated with POWHEG-V2 `two-rad`, with NLO (QCD+EW) + (QCD+QED) PS accuracy, the latter obtained using again PHOTOS for the QED part (red line). We dub the last approximation $\mathrm{QCD_{NLOPS}}\times\mathrm{EW_{NLOPS}}$. In the lower plots of figure 8 we show the relative impact of approximations *ii)* and *iii)* normalized to the pure QCD results of approximation *i)*. The relative effect of QED FSR corrections with LL accuracy on top of QCD corrected events (approximation *ii)*) is represented by the blue dots and it has already been shown in figure 7. The results of *iii)* include, beyond QED FSR corrections in LL approximation convoluted with QCD effects, the additional $\mathcal{O}(\alpha\alpha_s)$ corrections due to the NLO (QCD+EW) accuracy of POWHEG-V2 `two-rad`, matched with PHOTOS; their relative impact is expressed by the red dots. The difference between the red and the blue dots shows the impact, on the two observables under study, of the mixed QCD-EW corrections beyond the ones obtained with the convolution of QED FSR and QCD corrections; this difference is very small, at the per mille level or below, in both cases.

As a last point we investigate the effects of the different treatment of QED radiation between PHOTOS and PYTHIA-QED. In figures 9 and 10 we study the lepton-pair invariant mass and transverse mass distributions, and the lepton transverse momentum distribution. We show the ratio between the predictions obtained with PHOTOS and the ones with PYTHIA-QED in two different perturbative approximations: the QED FSR effects convoluted on top of the pure QCD POWHEG-V2 events (black dots) and these QED tools matched with the NLO (QCD+EW) accurate POWHEG-V2 `two-rad` code (blue dots). As it can be seen, the differences between PYTHIA and PHOTOS are not negligible for some specific observable, like e.g. the lepton-pair invariant mass, when the two tools are used stand-alone in convolution on top of the QCD events. This deviation from one is due to

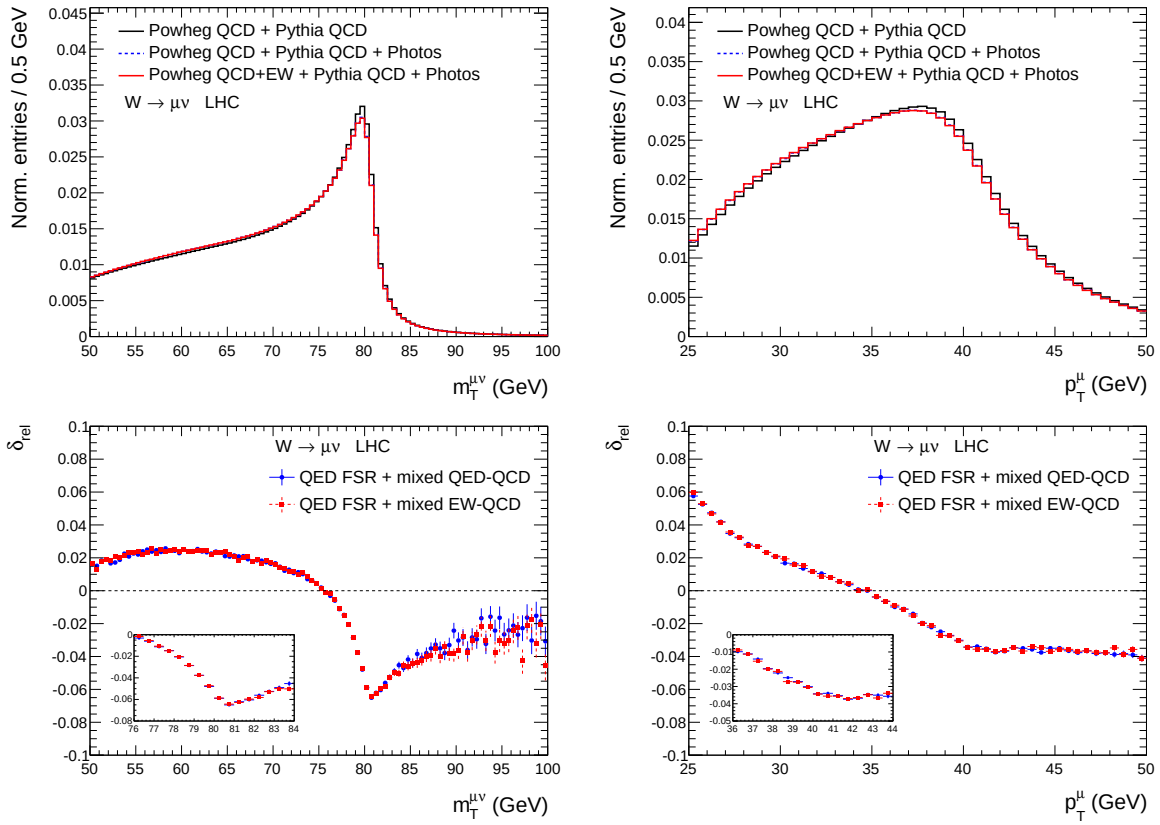
Norm. entries / 0.5 GeV
Powheg QCD + Pythia QCD
Powheg QCD + Pythia QCD + Photos
Powheg QCD+EW + Pythia QCD + Photos
W → μν LHC
$m_T^{\mu\nu}$ (GeV)
p_T^{μ} (GeV)
δ_{rel}
QED FSR + mixed QED-QCD
QED FSR + mixed EW-QCD

Figure 8. Upper plots: lepton-pair transverse mass (left plots) and lepton transverse momentum (right plots) distributions, for the decay $W^+ \to \mu^+\nu$ at the LHC 14 TeV, with acceptance cuts as in table 11, according to three different approximations: POWHEG-V2 with only QCD corrections, POWHEG-V2 with only QCD corrections interfaced to PHOTOS and POWHEG-V2 `two-rad` with NLO (QCD + EW) corrections matched to PHOTOS. Lower plots: relative contribution of QED FSR + mixed QCD-QED effects of the $\text{QCD}_{\text{NLOPS}}\times\text{QED}_{\text{PS}}$ approximation and of QED FSR + mixed QCD-EW corrections of the $\text{QCD}_{\text{NLOPS}}\times\text{EW}_{\text{NLOPS}}$ approximation, both normalized to the POWHEG-V2 with only QCD corrections results.

subleading terms of $\mathcal{O}(\alpha)$, which do not cancel in the ratio. The differences instead become negligible when PHOTOS and PYTHIA are matched with POWHEG-V2 `two-rad` with NLO (QCD+EW) accuracy. This better agreement is expected, because the first photon emission is now described with the exact matrix elements in both cases and differences start at $\mathcal{O}(\alpha^2)$ and are subleading, i.e. without a L_{QED} logarithmic enhancement. The same pattern as for the lepton-pair invariant mass can be observed in figure 10 for the lepton-pair transverse mass and lepton transverse momentum, but all the effects are smaller in size.

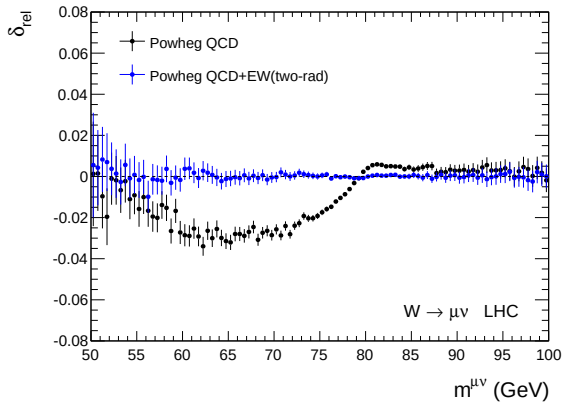

Figure 9. Comparison of different approximations of the $\mu^+\nu$ invariant mass distribution simulated at the LHC 14 TeV with acceptance cuts as in table 11. Relative difference of the predictions obtained with PHOTOS compared to the ones with PYTHIA-QED as tools to simulate QED FSR effects. The comparison is based on results computed with POWHEG-V2 with only QCD corrections interfaced to PHOTOS or PYTHIA-QED (black dots) and on results computed with POWHEG-V2 `two-rad` with NLO (QCD+EW) corrections, matched to PHOTOS or PYTHIA-QED (blue dots).

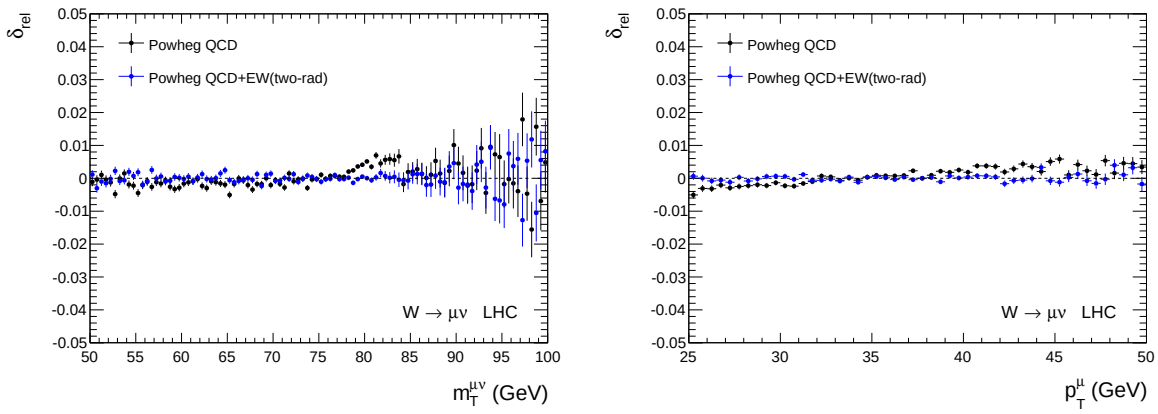

Figure 10. Same as in Figure 9 for the lepton-pair transverse mass (left plot) and for the lepton transverse momentum (right plot) distributions.

6 Impact of radiative corrections on the M_W determination

6.1 Template fitting method and simulation details

At the Tevatron, the W-boson mass is determined by a template fit to the lepton-pair transverse mass (M_T), charged lepton transverse momentum (p_T^l) or missing transverse energy ($\not{E}_T$) distributions, and a similar strategy is being implemented at the LHC. In this procedure, distributions are generated assuming a given theoretical model, for different values of M_W, and compared to data. The value of M_W is extracted as the one which gives the best agreement between the predicted and measured distributions.

In order to propagate the effect of the different theoretical corrections to the M_W extraction, we use a procedure inspired by the experimental one described above. We work with large MC samples, generated with different theoretical options, and use one in order to generate "templates" (predicted distributions for different input values of M_W), and the others as "pseudo–data" (distribution that will be probed by the templates).

All the samples are initially generated with the same input value for the W-boson mass, namely $M_{W,0}$=80.398 GeV and a fixed value of the width, $\Gamma_W = 2.141$ GeV. In order to produce the templates, we perform a reweighting of the distributions, assuming that the only dependence on M_W comes from the relativistic Breit–Wigner shape of the W resonance:

$$\frac{d\sigma}{d\hat{s}} \propto \frac{1}{(\hat{s} - M_W^2)^2 + M_W^2 \Gamma_W^2} \quad , \tag{6.1}$$

where $\hat{s}$ is the reduced squared c.m. energy. Notice that this is correct as long as the distributions are generated at LO accuracy in the treatment of EW corrections (further QCD corrections do not change this dependence), as we do in practice in our study. The reweighting avoids producing a large number of MC samples with different M_W input values, which would take a prohibitively large amount of CPU time, given that the target precision requires samples with a size of the order of 10^9 events.

For a particular pseudo–data distribution (and hence, for a particular theoretical assumption), we extract a measured value of M_W as the minimum of the parabola obtained by fitting the χ^2 vs. M_W curve, whose points come from the comparison of each template with that pseudo–data distribution. The difference between this extracted value of M_W and $M_{W,0}$ provides an estimate of the effect introduced in the pseudo–data with respect to the theoretical setup used in the generation of the templates. In other words it is an estimate of the shift that one would obtain by fitting the real data with templates based on that specific theoretical option (instead of the one of the reference templates). The shift uncertainty comes from the statistics of the MC samples and is estimated from the rule $\Delta\chi^2 \equiv \chi^2 - \chi^2_{\rm min} = 1$.

Both for templates and pseudo-data, we consider normalized differential cross sections, as we are interested to derive information on the impact of the different theoretical approximations just due to shape differences.

We present results for W decaying into muons and electrons, providing results for bare muons and recombined (or dressed) electrons (unless specified otherwise). For dressed electrons, the lepton and photon three-momenta are recombined into an effective momentum $\mathbf{p}^{eff} = \mathbf{p}^e + \mathbf{p}^\gamma$ for each photon satisfying the condition $\Delta R_{e,\gamma} = \left(\Delta\eta^2_{e,\gamma} + \Delta\phi^2_{e,\gamma}\right)^{1/2} \leq 0.1$, where $\Delta\phi_{e,\gamma}$ is the lepton-photon separation angle in the transverse plane. We focus on W^+ production and decays, but for a particular case (LHC setup), we show also results for W^-, in order to discuss the differences between the two cases.

In analogy to the Tevatron strategy, we perform template fits on the M_T and p_T^l distributions ($M_T \equiv \left(2\, p_T^\ell\, p_T^\nu\, [1 - \cos\Delta\phi_{\ell,\nu}]\right)^{1/2}$), using the following fit windows:

$$50 \text{ GeV} \leq M_T \leq 100 \text{ GeV}, \quad 27.5 \text{ GeV} \leq p_T^\ell \leq 47.5 \text{ GeV} \tag{6.2}$$

The distributions are obtained with a bin separation of 0.5 GeV. Only for the comparison of the effect of mixed QCD-EW corrections with fixed order result (section 6.4.1), we use a different setup, specified therein.

The template fitting procedure explained above is applied by taking into account typical acceptance cuts and using events at particle (or generator) level, in accordance with the Tevatron analyses and preliminary studies for the measurement of the W mass at the LHC. The details of the event selection and parameters are given in the following subsections.

Notice that the specific choice of the PDFs sets and of the factorization/renormalization scale is irrelevant for the study of purely EW effects on M_W, the theoretical contributions under scrutiny here being independent of those QCD details. In the case of mixed QCD-EW effects, these choices enter as a higher-order correction.

The results of the template fit procedure depend on the approximation used to compute the templates. In the following we consider two different options: templates computed at LO, without any radiative effect either of QCD or EW origin, and templates computed using the standard POWHEG-V2 with only QCD NLO corrections matched with the PYTHIA QCD PS. The second option provides a sensible approximation of the shape of the observables and in turn allows the assessment of the impact of higher-order corrections on the M_W determination.

6.2 QED, EW and lepton-pair corrections

The results of this section are obtained using HORACE. The distributions are computed at LO accuracy in QCD, in accordance with the procedure adopted at the Tevatron for the assessment of the QED/EW uncertainties, and include different subsets of EW corrections. The generation of events has been performed using MRST2004QED [108] as PDFs set, with factorization scale $\mu_F = M_{\ell\nu(\gamma)}$, where $M_{\ell\nu(\gamma)}$ is the invariant mass of the decaying W boson. In table 2 we summarize the event selection used for this part of the analysis. In table 3 we show the W mass shifts induced by QED and EW contributions at different

Process	$pp \to W^+ \to \mu^+\nu$, $\sqrt{s} = 14$ TeV
PDF	MRST2004QED
Event selection	$\lvert\eta^\ell\rvert < 2.5$, $p_T^\ell > 20$ GeV, $p_T^\nu > 20$ GeV

Table 2. Event selection used for the study of pure EW and QED effects.

accuracy levels, for bare muons and electrons. The last line contains results derived from PHOTOS as QED tool on top of the LO events generated with HORACE. The templates are at LO accuracy. In general, one can see that for the two most important observables, i.e. M_T and p_T^ℓ, the shifts are of similar size, of the order of 100 MeV for muons and 200 MeV for bare electrons. This is just a direct consequence of the fact that the EW corrections, dominated by QED FSR, give to M_T and p_T^ℓ a very similar relative effect, when normalized to the LO predictions, as it can be observed in section 5.3 in figure 7 in the lower plots, with the blue dots. Notice that these differences, obtained for LHC energies, are valid to a large extent for the Tevatron as well. Actually, the QED and lepton-pair corrections to the

	$pp \to W^+$, $\sqrt{s} = 14$ TeV Templates accuracy: LO Pseudo–data accuracy	M_W shifts (MeV) $W^+ \to \mu^+\nu$		$W^+ \to e^+\nu$	
		M_T	p_T^ℓ	M_T	p_T^ℓ
1	HORACE only FSR-LL at $\mathcal{O}(\alpha)$	-94±1	-104±1	-204±1	-230±2
2	HORACE FSR-LL	-89±1	-97±1	-179±1	-195±1
3	HORACE NLO-EW with QED shower	-90±1	-94±1	-177±1	-190±2
4	HORACE FSR-LL + Pairs	-94±1	-102±1	-182±2	-199±1
5	PHOTOS FSR-LL	-92±1	-100±2	-182±1	-199±2

Table 3. W mass shifts (in MeV) due to different QED/EW contributions and lepton-pair radiation, for muons and bare electrons at 14 TeV LHC. The templates are computed at LO without any shower correction, the pseudodata with the accuracy and the QED effects as indicated in the table.

determination of the W mass are in practice independent of the nominal c.m. energy. This feature follows from the fact that these theoretical contributions are driven by logarithmic terms of the form $L_{\rm QED} = \ln(\hat{s}/m_\ell^2)$, where m_ℓ is the mass of the radiating particle. Independently of the accelerator energy, the configurations with $\hat{s} \simeq M_W^2$, the W resonance, dominate the cross section and the kinematical distributions relevant for the determination of M_W.

Comparing the different lines of table 3, it can be noticed that:

- 1 vs. 2: the contribution due to multiple photon emission, beyond $\mathcal{O}(\alpha)$, dominated by two-photon radiation terms, amounts to some MeV for muons and to about 20 - 30 MeV for bare electrons, because of the very different impact of lepton-mass dependent collinear logarithms $L_{\rm QED}$. This is in agreement with previous studies at Tevatron energies, where the contribution of multiple FSR is taken into account using PHOTOS.

- 2 vs. 3: the contribution of non-logarithmic NLO EW corrections is a small effect, at a few MeV level, for both muons and electrons, and independent of the considered observable. This result emphasizes the dominant rôle played by QED FSR at LL level within the full set of NLO EW corrections.

- 2 vs. 4: the $\mathcal{O}(\alpha^2)$ contribution due to lepton-pair radiation induces a shift of M_W of about 5±1 MeV for muons and 3±1 MeV for electrons, when considering the fits to the transverse mass distribution. It is a not negligible effect given the present accuracy of the measurement at the Tevatron, where it is presently treated as a contribution to the QED uncertainty, because the PHOTOS version included in the Tevatron analyses did not simulate pair radiation[††]. For W decays into muons, the shift is of the same order of the one induced by multiple photon emission, whereas

[††] At present a version of PHOTOS including the effects of light-pair radiation is available, as described in ref. [77].

for W decays into bare electrons it is much smaller than multiple FSR. The lepton-flavor dependence of the pair radiation correction is a direct consequence of the $\beta_f(s), f = e, \mu$, expressions given in section 3.2 and, in turn, of the distortion of the kinematical distributions shown in section 5.1. As remarked in section 5.1, the recombination procedure reduces the impact of multiple photon radiation on dressed electrons, but does not modify the contribution of additional soft light pairs which instead are not recombined and constitute the largest fraction of the emitted pairs. Therefore, the 3 MeV shift due to pairs applies to both bare and dressed electrons.

- 2 vs. 5: the predictions of HORACE-3.1 and PHOTOS for the shifts due to multiple QED FSR agree at $\simeq 3 \pm 1$ MeV both for M_T and p_T^l, both in muon and electron final states. This agreement is certainly satisfactory, given the LL approximation inherent in the two programs.

The comparison of HORACE-3.1 and PHOTOS in lines 2 and 5 tests the *technical* precision of the two codes, which claim the same accuracy but differ by subleading terms and in the implementation of the generation of radiation. An estimate of the *physical* precision of PHOTOS, instead, can be obtained with a comparison of its results against those of the a code that includes a more complete set of higher-order radiative corrections. Since PHOTOS does not include exact NLO EW corrections nor the effect of lepton-pair radiation, we can derive the size of these effects within the HORACE-3.1 framework from the comparison of line 2 with lines 3 and 4 of table 3. By summing the two sources in quadrature, we conclude that the uncertainty of a QED modeling based on PHOTOS is in the range $4 - 6 \pm 1$ MeV both for M_T and p_T^ℓ, and it is independent of the final state lepton flavor. This conclusion is in agreement with the estimates of the QED uncertainty presently provided by CDF and DØ collaborations, which make use of a procedure very similar to the one here described.

6.3 EW input scheme variation

We compare now the shifts due to the choice of the input parameter scheme, to provide an estimate of the theoretical uncertainty of EW origin at NNLO accuracy. Indeed, as already emphasized, a complete calculation of the NNLO EW corrections to DY processes is presently unavailable. The results in table 4 correspond to the three different input schemes introduced in section 4.1 and come from simulations both at NLO and in the NLO+PS formulation of HORACE-3.1 at the Tevatron energy. All the numbers in table 4 are computed using the same templates with LO accuracy without any QCD correction, neither fixed-order nor from Parton Shower. The details of the event generation and selection are given in table 5.

The main comments are the following.

- When considering NLO predictions (lines 1, 2 and 3), the shifts are not negligible, reaching the 10 MeV level. They are induced by the different $\mathcal{O}(\alpha^2)$ components present in the three schemes.

- However, the shifts are considerably reduced, down to about 1–2 MeV, when NLO corrections are matched with higher–order contributions (lines 4, 5 and 6). This

	$p\bar{p} \to W^+$, $\sqrt{s} = 1.96$ TeV Templates accuracy: LO Pseudodata accuracy	Input scheme	M_W shifts (MeV) $W^+ \to \mu^+\nu$ M_T	 p_T^ℓ
1	HORACE NLO-EW	α_0	-101±1	-117±2
2		$G_\mu - I$	-112±1	-130±1
3		$G_\mu - II$	-101±1	-117±1
4	HORACE NLO-EW+QED-PS	α_0	-70±1	-81±1
5		$G_\mu - I$	-72±2	-83±1
6		$G_\mu - II$	-72±1	-82±2

Table 4. W mass shifts (in MeV) induced by different input scheme choices, at NLO-EW (lines 1, 2 and 3) and NLO-EW+ QED-PS (lines 4, 5 and 6) accuracy, for the muon channel, at the Tevatron with $\sqrt{s} = 1.96$ TeV. The templates have been computed at LO without any shower correction.

Process	$p\bar{p} \to W^+ \to \mu^+\nu$, $\sqrt{s} = 1.96$ TeV
PDF	MRST2004QED
Event selection	$\lvert\eta^\ell\rvert < 1.05$, $p_T^\ell > 25$ GeV, $p_T^\nu > 25$ GeV

Table 5. Event selection used for the study of the EW input scheme variation.

follows from the fact that the sharing of the different photon multiplicities is the same in the three schemes, as remarked in Section 4.1.

- The α_0 and the $G_\mu - II$ schemes behave in a very similar way, as it can be clearly noticed from the results of the $\mathcal{O}(\alpha)$ analysis (line 2). This result is a consequence of the equality of the relative fraction of the 0– and 1–photon samples in the two cases.

- Since both versions of the G_μ scheme are *a priori* acceptable in the absence of a complete NNLO EW calculation, it follows from the results shown in line 6 that there is an intrinsic input scheme arbitrariness that induces an uncertainty on the W mass at the 1 MeV level.

In summary, the uncertainty due to missing NNLO EW corrections, as estimated through input scheme variation, is at the MeV level and could be further reduced only with a complete $\mathcal{O}(\alpha^2)$ calculation.

6.4 Mixed QCD-EW corrections

In this section we study the M_W shift induced by mixed QCD-EW corrections, in different perturbative approximations. In section 6.4.1 we compare the size of the M_W shift induced by mixed the $\mathcal{O}(\alpha\alpha_s)$ corrections present in our theoretical formulation, based on POWHEG-V2 `two-rad` with NLO (QCD+EW) accuracy, with the results available in the literature, obtained with the fixed-order calculation in pole approximation [94–97]. In sections (6.4.2-6.4.3) we systematically compare two different approximations available in POWHEG-V2: *i)* we consider distributions computed with $\text{QCD}_{\text{NLOPS}} \times \text{QED}_{\text{PS}}$ approximation and use,

as a tool that simulates QED FSR effects, either PHOTOS or PYTHIA-QED; *ii)* we generate distributions in $\mathrm{QCD_{NLOPS}}\times\mathrm{EW_{NLOPS}}$ approximation, using POWHEG-V2 `two-rad` with NLO (QCD+EW) accuracy and matched with PYTHIA as QCD PS and with PHOTOS or PYTHIA-QED as QED PS. The comparison of these two approximations offers some hints for a critical assessment of the theoretical uncertainty induced by mixed QCD-EW corrections. This contribution is presently neglected in the theoretical error estimate by the Tevatron collaborations, but it can be nonetheless evaluated, using the state of the art of theoretical tools. Eventually, in section 6.4.4 we comment on the impact on the M_W determination of the upgrade `two-rad` with respect to the previous public versions of POWHEG-V2 with NLO (QCD+EW) accuracy.

Unless stated otherwise, the templates used in the fitting procedure have been computed with the standard POWHEG-V2 version that includes only QCD corrections, namely with NLO QCD accuracy and matched with PYTHIA8 for the simulation of multiple parton QCD ISR. The simulations have been done using MSTW2008 NLO [108] as PDFs set, with factorization/renormalization scale $\mu_F = \mu_R = M_{\ell\nu(\gamma)}$. For the separation between Btilde and Remnant contributions, we use the default setting, which means that a radiative contribution is considered remnant if the ratios between the full matrix element and its soft/collinear approximations are greater than five. For the simulation of QED FSR, we use both PYTHIA8 and PHOTOS version 3.56, the latter without QED matrix element corrections.

6.4.1 Comparisons with fixed-order results

In this section we focus on the study of the lepton-pair transverse mass distribution and we compare the W mass shifts induced by the mixed QCD-EW corrections contained in the POWHEG-V2 `two-rad` predictions with the ones based on the fixed-order results of refs. [96, 97]. As already discussed in Section 4.2, the factorized approach implemented in POWHEG-V2 `two-rad` contains part of the $\mathcal{O}(\alpha\alpha_s)$ terms. Actually, through the use of QCD and QED parton showers, terms of $\mathcal{O}(\alpha_s^m\alpha^n)$, with $m, n \geq 1$, are included to all orders as well. This means, strictly speaking, that a comparison with the fixed-order results of refs. [96, 97] is not possible. However, for the M_T distribution, QCD corrections have a mild impact on the distribution, as remarked in section 5.3; we can thus assume that the dominant part of the mixed corrections is given by the lowest order term with $m = n = 1$, with negligible effects from higher-order terms. In order to comply with refs. [96, 97], we adopt the event selection and fit setup used there, as detailed in table 6. The templates used in this comparison, at variance with the rest of section 6.4, are generated with LO accuracy.

In order to isolate a contribution that can be compared to the one obtained in refs. [96, 97], we observe that the perturbative content, with respect to the LO prediction, of the fully differential POWHEG result, including showering effects, can be cast in the following form:

$$d\sigma_{\mathrm{POWHEG}} = d\sigma_0 \left[1 \; + \; \delta_{\alpha_s} + \delta_{\alpha} + \sum_{m=1,n=1}^{\infty} \delta'_{\alpha_s^m\alpha^n} + \sum_{m=2}^{\infty} \delta'_{\alpha_s^m} + \sum_{n=2}^{\infty} \delta'_{\alpha^n} \right], \tag{6.3}$$

Process	$pp \to W^+ \to \mu^+\nu$, $\sqrt{s} = 14$ TeV
PDF	MSTW2008 NLO
Event selection	$\lvert\eta^\ell\rvert < 2.5$, $p_T^\ell > 25$ GeV, $p_T^\nu > 25$ GeV
Fit window	64 GeV $\leq M_T \leq$ 91 GeV
Bin width of M_T distribution	1 GeV

Table 6. Event selection and fit setup used for the comparison with the fixed order results of refs.[94–97].

	Templates	Pseudodata	M_W shifts (MeV)
1	LO	POWHEG(QCD) NLO	56.0 ± 1.0
2	LO	POWHEG(QCD)+PYTHIA(QCD)	74.4 ± 2.0
3	LO	HORACE(EW) NLO	-94.0 ± 1.0
4	LO	HORACE (EW,QEDPS)	-88.0 ± 1.0
5	LO	POWHEG(QCD,EW) NLO	-14.0 ± 1.0
6	LO	POWHEG(QCD,EW) `two-rad`+PYTHIA(QCD)+PHOTOS	-5.6 ± 1.0

Table 7. W mass shift (in MeV) induced by different sets of perturbative corrections and evaluated with templates computed at LO, at the LHC 14 TeV for $\mu^+\nu$ production.

correction factor in eq. 6.3	samples in table 7	M_W shift (MeV)
$\sum_{m=1,n=1}^{\infty} \delta'_{\alpha_s^m\alpha^n} + \sum_{m=2}^{\infty} \delta'_{\alpha_s^m} + \sum_{n=2}^{\infty} \delta'_{\alpha^n}$	[6]-[5]	8.4 ±1.4 MeV
$\sum_{m=2}^{\infty} \delta'_{\alpha_s^m}$	[2]-[1]	18.4 ±2.2 MeV
$\sum_{n=2}^{\infty} \delta'_{\alpha^n}$	[4]-[3]	6.0 ±1.4 MeV

Table 8. Impact in terms of M_W shifts of the correction factors present in eq. 6.3, contributing to the POWHEG-V2 `two-rad` simulations with NLO (QCD+EW) accuracy, derived from the results of table 7.

where the factors δ represent the correction, normalized to the LO result, induced by different subsets of higher-order terms, the latter labelled by the indices. We add a prime to those δ factors where the corresponding correction is not known exactly but it is only approximated. We extract the contribution to the W mass shift given by $\sum_{m=1,n=1}^{\infty} \delta'_{\alpha_s^m\alpha^n}$ in eq. 6.3, subtracting from the full result the shift induced by the NLO contribution $(\delta_{\alpha_s} + \delta_\alpha)$ and the one of the higher-order contributions $\sum_{m=2}^{\infty} \delta'_{\alpha_s^m}$ and $\sum_{n=2}^{\infty} \delta'_{\alpha^n}$.

For this analysis we generate pseudodata samples with different perturbative accuracies, including: 1) only fixed-order NLO QCD; 2) NLO QCD matched with QCD PS; 3) only fixed-order NLO EW corrections; 4) NLO EW matched with QED PS; 5) only fixed-order NLO (QCD+EW); 6) NLO (QCD+EW) matched with (QCD+QED) PS. In table 7 we present the shifts associated to these 6 samples, extracted with templates computed at LO, while in table 8 we show the combinations relevant for the determination of $\sum_{m=1,n=1}^{\infty} \delta'_{\alpha_s^m\alpha^n}$. Subtracting the second and third lines from the first line of table 8 we obtain our estimate for the shift $\Delta {M_W}^{\alpha_s\alpha}$ induced by the correction factor $\sum_{m=1,n=1}^{\infty} \delta'_{\alpha_s^m\alpha^n}$,

which turns out to be

$$\Delta M_W{}^{\alpha_s \alpha} = -16.0 \pm 3.0 \text{ MeV},$$

in nice agreement with $\delta_{\rm NNLO} = -14$ MeV of refs. [96, 97].

From table 7 we can obtain additional information. We remark that the shift induced by NLO QCD corrections is positive and sizeable, 56 ± 1 MeV. Given the large cancellation of the NLO QCD and NLO EW corrections at the jacobian peak of the M_T distribution, which is illustrated in figure 4, and given also the non-linear behaviour of the χ^2 function in the fitting procedure, we observe that the shift extracted from sample 5, namely with the simultaneous presence of NLO QCD and NLO EW effects, is different from the sum of the two shifts obtained with one set of corrections at a time (samples 1 and 3).

6.4.2 Results for the Tevatron

In this section we focus on W production at the Tevatron. The details of the event selection are shown in table 9 and we notice the introduction of a cut in the transverse momentum of the W boson (p_T^W), defined as $p_T^W \equiv |\mathbf{p}_T^\ell + \mathbf{p}_T^\nu + \sum \mathbf{p}_T^\gamma|$, where the sum runs on all the photons emitted by the charged lepton. As already anticipated, here and in the following

Process	$p\bar{p} \to W^+ \to \mu^+\nu$, $\sqrt{s} = 1.96$ TeV
PDF	MSTW2008 NLO
Event selection	$\lvert\eta^\ell\rvert < 1.05$, $p_T^\ell > 25$ GeV, $p_T^\nu > 25$ GeV, $p_T^W < 15$ GeV

Table 9. Event selection used for the study of QED and mixed QCD-EW effects at Tevatron.

sections we consider the following two approximations: *i)* $\text{QCD}_{\text{NLOPS}} \times \text{QED}_{\text{PS}}$ using either PHOTOS or PYTHIA-QED to simulate QED FSR effects, *ii)* $\text{QCD}_{\text{NLOPS}} \times \text{EW}_{\text{NLOPS}}$ using again either PHOTOS or PYTHIA-QED to simulate QED FSR effects. In table 10 we present the corresponding shifts (lines 1 and 2 for approximation *i)*, lines 3 and 4 for approximation *ii)*). We can notice that:

	$p\bar{p} \to W^+$, $\sqrt{s} = 1.96$ TeV Templates accuracy: NLO-QCD+QCD_{PS} Pseudodata accuracy	QED FSR	M_W shifts (MeV) $W^+ \to \mu^+\nu$		$W^+ \to e^+\nu$(dres)	
			M_T	p_T^ℓ	M_T	p_T^ℓ
1	NLO-QCD+$(\text{QCD+QED})_{\text{PS}}$	PYTHIA	-91±1	-308±4	-37±1	-116±4
2	NLO-QCD+$(\text{QCD+QED})_{\text{PS}}$	PHOTOS	-83±1	-282±4	-36±1	-114±3
3	NLO-(QCD+EW)-`two-rad`+$(\text{QCD+QED})_{\text{PS}}$	PYTHIA	-86±1	-291±3	-38±1	-115±3
4	NLO-(QCD+EW)-`two-rad`+$(\text{QCD+QED})_{\text{PS}}$	PHOTOS	-85±1	-290±4	-37±2	-113±3

Table 10. W mass determination for muons and dressed electrons at the Tevatron. M_W shifts (in MeV) due to multiple QED FSR and mixed QCD-EW corrections, computed with PYTHIA-QED and PHOTOS as tools for the simulation of QED FSR effects. PYTHIA-QED and PHOTOS have been interfaced to POWHEG-V2 with only QCD corrections (lines 1 and 2) or matched to POWHEG-V2 `two-rad` with NLO (QCD+EW) accuracy (lines 3 and 4). The templates have been computed with POWHEG-V2 with only QCD corrections. The results are based on MC samples with 1×10^8 events.

- 1 vs. 2: there is a not negligible difference between the predictions of PYTHIA-QED and PHOTOS for the QED FSR contribution. These differences amount to about 8 ± 1 MeV for the lepton-pair transverse mass and to about 26 ± 5 MeV for the lepton p_T^l for muons and disappear for dressed electrons. The origin of the difference in size for the two observables has been discussed in section 5.2 and derives from the different modeling of QED radiation in the two programs. The impact of this difference on the observables relevant for the M_W determination has been shown in figure 10 (black dots). Notice that this difference is robust, as we carefully checked that the parameters and theoretical ingredients used in our PYTHIA-QED simulations are fully consistent with those of PHOTOS (same value of the electromagnetic coupling constant given by $\alpha(0)$, no pair radiation and negligible effect of QED ISR in PYTHIA-QED).

- 3 vs. 4: the shifts induced by mixed $\mathcal{O}(\alpha\alpha_s)$ corrections are independent of the QED radiation model, or, in other words, the effect of QED terms subleading in an expansions in powers of $L_{\rm QED}$ is negligible. In fact the shifts of lines 3 and 4 agree at the level of 1 MeV, within the statistical error, both for M_T and p_T^l in the case of muons and dressed electrons. This can be understood by the fact that the hardest QED final state photon is described, in both approaches, with NLO matrix element accuracy and the QED LL shower simulates only higher-order effects. As a consequence, the differences stemming from different QED simulations between PYTHIA-QED and PHOTOS start from $\mathcal{O}(\alpha^2)$. The differences for both lepton-pair transverse mass and lepton transverse momentum distributions are at the 0.1% level, as shown in figure 10 (blue dots) and flat around the jacobian peak, yielding differences in the M_W shifts below the 1 MeV target uncertainty.

- 1 vs. 3 and 2 vs. 4: the difference between these theoretical options provides an estimate of the contribution of mixed $\mathcal{O}(\alpha\alpha_s)$ corrections, that are not included in the stand-alone tools that simulate QED FSR and that become available only after matching these tools with an exact NLO EW calculation.

  We note that the estimate of the mixed $\mathcal{O}(\alpha\alpha_s)$ corrections depends on the tool used to simulate QED FSR. In particular, the estimate of these effects with FSR simulated with PYTHIA-QED amounts to a $\sim 5 \pm 1$ MeV shift for the lepton-pair transverse mass and to a shift of the order of $\sim 17 \pm 5$ MeV for the lepton transverse momentum, in the case of muons; for recombined electrons the shifts are of the size of $\sim 1 \pm 1$ MeV and $\sim 1 \pm 5$ MeV for M_T and p_T^l, respectively. When simulating QED FSR with PHOTOS the effects amount to a $\sim 2 \pm 1$ MeV shift for the transverse mass and to a shift of the order of $\sim 8 \pm 5$ MeV for the lepton transverse momentum, in the case of muons; for recombined electrons the shifts are of the size of $\sim 1 \pm 2$ MeV and $\sim 1 \pm 4$ MeV for M_T and p_T^l, respectively.

  These results show that a QED-LL approach without matching is more accurate, at the level of precision required for the M_W determination, when QED FSR is simulated with PHOTOS (line 2). The small difference between the shifts obtained

with PHOTOS with and without matching with the NLO EW results can also be understood from figure 8, where the relative impact of the EW effects in the two cases is almost identical.

These comparisons can be considered as a measure of the accuracy inherent in the use of a generator given by a tandem of tools like RESBOS+PHOTOS (like in the present Tevatron measurements) in the sector of mixed QCD-EW corrections.

The assessment of the uncertainty for the Tevatron as explained in the third item above, is, in our opinion, one of the most important and original aspects of our study.

6.4.3 Results for the LHC

In this section we present the results for a similar analysis to the one addressed in Section 6.4.2, but under LHC conditions. The details of the event selection are shown in table 11, and the corresponding mass shifts in table 12.

Process	$pp \to W^+ \to \mu^+\nu$, $\sqrt{s} = 14$ TeV
PDF	MSTW2008 NLO
Event selection	$\lvert\eta^\ell\rvert < 2.5$, $p_T^\ell > 20$ GeV, $p_T^\nu > 20$ GeV, $p_T^W < 30$ GeV

Table 11. Event selection used for the study of QED and mixed QCD-EW effects at LHC.

	$pp \to W^+$, $\sqrt{s} = 14$ TeV Templates accuracy: NLO-QCD+QCD_{PS} Pseudodata accuracy	QED FSR	M_W shifts (MeV) $W^+ \to \mu^+\nu$ M_T	 p_T^ℓ	 $W^+ \to e^+\nu$(dres) M_T	 p_T^ℓ
1	NLO-QCD+$(\text{QCD+QED})_{\text{PS}}$	PYTHIA	-95.2±0.6	-400±3	-38.0±0.6	-149±2
2	NLO-QCD+$(\text{QCD+QED})_{\text{PS}}$	PHOTOS	-88.0±0.6	-368±2	-38.4±0.6	-150±3
3	NLO-(QCD+EW)+$(\text{QCD+QED})_{\text{PS}}$`two-rad`	PYTHIA	-89.0±0.6	-371±3	-38.8±0.6	-157±3
4	NLO-(QCD+EW)+$(\text{QCD+QED})_{\text{PS}}$`two-rad`	PHOTOS	-88.6±0.6	-370±3	-39.2±0.6	-159±2

Table 12. W mass determination for muons and dressed electrons at the LHC 14 TeV in the case of W^+ production. M_W shifts (in MeV) due to multiple QED FSR and mixed QCD-EW corrections, computed with PYTHIA-QED and PHOTOS as tools for the simulation of QED FSR effects. PYTHIA-QED and PHOTOS have been interfaced to POWHEG-V2 with only QCD corrections (lines 1 and 2) or matched to POWHEG-V2 `two-rad` with NLO (QCD+EW) accuracy (lines 3 and 4). The templates have been computed with POWHEG-V2 with only QCD corrections. The results are based on MC samples with 4×10^8 events.

Similar remarks on the comparison between PYTHIA-QED and PHOTOS, as well as on mixed QCD-EW corrections, apply in this case. However, further considerations can be drawn by comparing the results of table 12, where QCD corrections are included with NLO QCD + QCD PS accuracy, with those in table 3, which correspond to LHC simulations in the same setup but at LO accuracy in QCD. In particular, this comparison is meaningful for the W mass shifts obtained with PHOTOS for the modeling of QED FSR in table 12. One can notice that:

- By comparing the results with muons, in the last line of table 3 with those in the second line of table 12, the shift is largely independent of the presence of QCD corrections for fits to the lepton-pair transverse mass, whereas the shift extracted from the lepton transverse momentum distribution is strongly influenced by the inclusion of QCD contributions.

  As it has been discussed in section 5.3 and shown in figure 7, QCD corrections preserve to a large extent the LO shape of the lepton-pair transverse mass and strongly modify the LO shape of the lepton transverse momentum distributions. In the latter case, the broader shape enhances the impact of radiative corrections in the template fit procedure. The large corrections induce in turn large mixed QCD-QED effects, which contribute to the differences between tables 3 and 12.

- 1 vs. 3 and 2 vs. 4: as a consequence of the above point, the effect due to mixed QCD-EW corrections, beyond those due to QED FSR, is of the same order at Tevatron and the LHC for fits to M_T, while they are enhanced at the LHC for fits to p_T^ℓ. As already noticed in the analysis for the Tevatron, in the case of the lepton transverse momentum these effects depend on the model of QED FSR. If we consider PYTHIA-QED, the M_W shift is in the range $\sim 29\pm5$ MeV for p_T^ℓ with muons (even if, considering the associated numerical uncertainty, LHC and Tevatron results could be compatible). If QED FSR is instead simulated with PHOTOS, the mixed QCD-EW corrections are already well accounted for by the convolution of PHOTOS stand-alone with the events generated with NLO QCD + QCD PS accuracy, with an uncertainty at the MeV level.

- 1 vs. 2: as at the Tevatron, there are differences between the predictions of PYTHIA-QED and PHOTOS for QED FSR for muons under a bare event selection, which however disappear when considering dressed electrons or, in full generality, disappear after matching with an exact NLO EW calculation (lines 3 and 4).

In order to summarize the results shown in section 6.4.2 and in the present section, we collect in table 13 the shifts induced on M_W (as extracted from the M_T or p_T^ℓ distributions in the case of W^+ production, with bare muon event selections, at Tevatron and LHC) by the subset of mixed QCD-EW corrections present in $\text{QCD}_{\text{NLOPS}}\times\text{EW}_{\text{NLOPS}}$ but not included in $\text{QCD}_{\text{NLOPS}}\times\text{QED}_{\text{PS}}$ approximation. As a reference, we remind that, by inspection of the shifts as in the last line of table 3 (QED FSR effects) in comparison with those in the second line of table 12 (QED FSR and mixed QCD-QED effects), the M_W shift due to mixed QCD-QED factorized effects amounts to $+4\pm1$ MeV for fits to the transverse mass and QED FSR simulated with PHOTOS.

We show in table 14 results for the process $pp \to W^- \to \ell^-\nu$ at LHC energies, to be compared with the results for W^+ production in table 12. In this case, the parameters and event selection are the same as those shown in table 11. From lines 3 and 4 of table 14 we remark that in $\text{QCD}_{\text{NLOPS}}\times\text{EW}_{\text{NLOPS}}$ approximation the mixed QCD-EW effects due to a different modeling of QED FSR are at the 1 MeV level, as in the W^+ case. The comparison between lines 1 and 3 and between lines 2 and 4 shows the

		ΔM_W(MeV)	
	QED FSR model	M_T	p_T^ℓ
Tevatron	PYTHIA	+5 ± 2	+17 ± 5
	PHOTOS	-2 ± 1	-8 ± 5
LHC	PYTHIA	+6.2 ± 0.8	+29 ± 4
	PHOTOS	-0.6 ± 0.8	-2 ± 4

Table 13. Residual M_W shifts computed as the difference of the results of the simulations with $\text{QCD}_{\text{NLOPS}}\times\text{EW}_{\text{NLOPS}}$ and $\text{QCD}_{\text{NLOPS}}\times\text{QED}_{\text{PS}}$ accuracy, with PYTHIA-QED and PHOTOS, for Tevatron and LHC 14 TeV energies, in the case of W^+ production and bare muons.

impact of mixed QCD-EW corrections present in $\text{QCD}_{\text{NLOPS}}\times\text{EW}_{\text{NLOPS}}$ but absent in $\text{QCD}_{\text{NLOPS}}\times\text{QED}_{\text{PS}}$: while PHOTOS stand-alone provides already a good approximation of the NLO results (lines 2 and 4), the results of PYTHIA-QED stand-alone differ with respect to those with $\text{QCD}_{\text{NLOPS}}\times\text{EW}_{\text{NLOPS}}$ accuracy (lines 1 and 3); we also remark that in the PYTHIA-QED case the difference of the shifts is larger than the corresponding one in the W^+ case and reaches 34 MeV for the muon transverse momentum distribution. Although the statistics is not sufficient to draw a firm conclusion about a different behaviour of W^+ and W^-, our results suggest that the evaluation of the theoretical shifts and related uncertainties requires at the LHC a separate study of W^- and W^+ production and decay, at least for the lepton p_T^l.

	$pp \to W^-$, $\sqrt{s} = 14$ TeV Templates accuracy: NLO-QCD+QCD_{PS} Pseudodata accuracy	QED FSR	M_W shifts (MeV) $W^- \to \mu^-\bar{\nu}$ M_T	 p_T^ℓ	 $W^- \to e^-\bar{\nu}$(dres) M_T	 p_T^ℓ
1	NLO-QCD+$(\text{QCD+QED})_{\text{PS}}$	PYTHIA	-97±1	-413±4	-39±1	-155±4
2	NLO-QCD+$(\text{QCD+QED})_{\text{PS}}$	PHOTOS	-90±1	-379±5	-40±1	-154±5
3	NLO-(QCD+EW)+$(\text{QCD+QED})_{\text{PS}}$`two-rad`	PYTHIA	-90±1	-379±5	-40±1	-166±5
4	NLO-(QCD+EW)+$(\text{QCD+QED})_{\text{PS}}$`two-rad`	PHOTOS	-89±1	-377±4	-40±1	-164±4

Table 14. W mass determination for muons and dressed electrons at the LHC 14 TeV in the case of W^- production. M_W shifts (in MeV) due to multiple QED FSR and mixed QCD-EW corrections, computed with PYTHIA-QED and PHOTOS as tools for the simulation of QED FSR effects. PYTHIA-QED and PHOTOS have been interfaced to POWHEG-V2 with only QCD corrections (lines 1 and 2) or matched to POWHEG-V2 `two-rad` with NLO (QCD+EW) accuracy (lines 3 and 4). The templates have been computed with POWHEG-V2 with only QCD corrections. The results are based on MC samples with 1×10^8 events.

As a last remark, we stress that, aiming at an M_W determination with ∼MeV uncertainty, we have validated the description of mixed $\mathcal{O}(\alpha\alpha_s)$ contributions obtained in a $\text{QCD}_{\text{NLOPS}}\times\text{QED}_{\text{PS}}$ approximation with PHOTOS. If, on the contrary, QED FSR is described with PYTHIA-QED, the matching with NLO EW results in a $\text{QCD}_{\text{NLOPS}}\times\text{EW}_{\text{NLOPS}}$ approximation is needed.

6.4.4 Impact on M_W determination of the POWHEG-V2 `two-rad` improvement

In this section we discuss the impact on the M_W determination of the upgrade dubbed `two-rad` of the code POWHEG-V2 with NLO (QCD+EW) accuracy matched to (QCD+QED) PS, described in section 3.3.1, compared to the previous public versions of the code.

	$pp \to W^+$, $\sqrt{s} = 14$ TeV Templates accuracy: NLO-QCD+QCD$_{\rm PS}$ Pseudodata accuracy	QED FSR	M_W shifts (MeV) $W^+ \to \mu^+\nu$ M_T	 p_T^ℓ	 $W^+ \to e^+\nu$(dres) M_T	 p_T^ℓ
1	NLO-QCD+(QCD+QED)$_{\rm PS}$	PYTHIA	-95.2±0.6	-400±3	-38.0±0.6	-149±2
2	NLO-QCD+(QCD+QED)$_{\rm PS}$	PHOTOS	-88.0±0.6	-368±2	-38.4±0.6	-150±3
3	NLO-(QCD+EW)+(QCD+QED)$_{\rm PS}$`two-rad`	PYTHIA	-89.0±0.6	-371±3	-38.8±0.6	-157±3
4	NLO-(QCD+EW)+(QCD+QED)$_{\rm PS}$`two-rad`	PHOTOS	-88.6±0.6	-370±3	-39.2±0.6	-159±2
5	NLO-(QCD+EW)+(QCD+QED)$_{\rm PS}$	PYTHIA	-101.8±0.4	-423±2	-45.0±0.6	-179±2
6	NLO-(QCD+EW)+(QCD+QED)$_{\rm PS}$	PHOTOS	-94.2±0.6	-392±2	-45.2±0.6	-181±2

Table 15. Analysis of the impact on the M_W determination of the `two-rad` upgrade of POWHEG-V2 with NLO (QCD+EW) accuracy (lines 3 and 4), compared to the older public versions (lines 5 and 6). All the parameters and specifications as in table 12.

	$p\bar{p} \to W^+$, $\sqrt{s} = 1.96$ TeV Templates accuracy: NLO-QCD+QCD$_{\rm PS}$ Pseudodata accuracy	QED FSR	M_W shifts (MeV) $W^+ \to \mu^+\nu$ M_T	 p_T^ℓ	 $W^+ \to e^+\nu$(dres) M_T	 p_T^ℓ
1	NLO-QCD+(QCD+QED)$_{\rm PS}$	PYTHIA	-91±1	-308±4	-37±1	-116±4
2	NLO-QCD+(QCD+QED)$_{\rm PS}$	PHOTOS	-83±1	-282±4	-36±1	-114±3
3	NLO-(QCD+EW)+(QCD+QED)$_{\rm PS}$`two-rad`	PYTHIA	-86±1	-291±3	-38±1	-115±3
4	NLO-(QCD+EW)+(QCD+QED)$_{\rm PS}$`two-rad`	PHOTOS	-85±1	-290±4	-37±2	-113±3
5	NLO-(QCD+EW)+(QCD+QED)$_{\rm PS}$	PYTHIA	-96±1	-323±3	-45±1	-129±3
6	NLO-(QCD+EW)+(QCD+QED)$_{\rm PS}$	PHOTOS	-89±1	-300±3	-44±2	-134±3

Table 16. Analysis of the impact on the M_W determination of the `two-rad` upgrade of POWHEG-V2 with NLO (QCD+EW) accuracy (lines 3 and 4), compared to the older public versions (lines 5 and 6). All the parameters and specifications as in table 10.

We stress that the new version `two-rad` superseeds the previous public versions and is the only version that must be used for physical analyses. As illustrated in figure 3, the `two-rad` version removes a double counting of QED FSR contributions and of mixed QCD-QED contributions; the latter, present in the previous versions of the code, causes a distortion at the jacobian peak of the shape of the lepton-pair transverse mass and lepton transverse momentum distributions. The distortion, visible by comparing the blue dots with respect to the red dots in figure 3, induces an additional shift of M_W, shown in table 15 where we repeat for convenience also the other values of table 12, computed with LHC conditions in the case of W^+ production. We can observe, by comparing lines 3 and 5 or lines 4 and 6, the shift of order -10 MeV induced on M_W extracted from the lepton-pair

transverse mass and the shift of about -25/-50 MeV induced on M_W extracted from the lepton transverse momentum distributions. A clear sign of the problems in the previous implementations emerges in the comparison of lines 5 and 6, because the dependence on the model that describes QED FSR, i.e. PYTHIA-QED vs. PHOTOS, is not reduced after matching with an exact NLO EW calculation and remains at the level of the comparison between lines 1 and 2, where, instead, a discrepancy is justified.

A similar behaviour of the previous versions of POWHEG-V2 with NLO (QCD+EW) accuracy has been observed also with the Tevatron setup and is illustrated in table 16.

7 Conclusions

In this paper, we have presented a comprehensive study of electroweak, QED and mixed factorizable QCD-electroweak corrections underlying the theoretical modeling necessary in the precise measurement of the W-boson mass at hadron colliders.

We have shown that particular attention must be paid in the treatment of QED FSR, as the models implemented in PYTHIA and PHOTOS give rise to different M_W shifts; the PHOTOS simulation of FSR is more reliable because it better approximates a matrix element behaviour and it has been validated with the HORACE-3.1 independent results.

We have shown that neglecting the contribution of light lepton pairs in the evaluation of the theoretical templates introduces an uncertainty (both for Tevatron and LHC) of $3-5\pm1$ MeV; the first value is for final state electrons, the second one applies to muons and the conclusion holds for fits both to M_T and p_T^l.

We have pointed out that mixed factorizable $\mathcal{O}(\alpha\alpha_s)$ corrections, as calculated by means of an improved version of POWHEG-V2 with QCD and EW corrections, i.e. POWHEG-V2 `two-rad`, induce a shift on M_W of -16 ± 3 MeV, in good agreement with the estimate of Ref. [96] based on a NNLO calculation in pole approximation. We have provided clear evidence that M_W shifts due to factorizable $\mathcal{O}(\alpha\alpha_s)$ corrections are largely dominated by the interplay between QCD radiation and QED FSR, the residual mixed corrections beyond the approximation $\mathrm{QCD_{NLOPS}}\times\mathrm{QED_{PS}}$ being very small, at the 1 MeV level. Again these results apply to M_T and p_T^l and are based on simulations generated with POWHEG-V2 `two-rad`.

The study of mixed QCD-EW corrections to DY processes motivated the development of the code POWHEG-V2 with NLO (QCD+EW) accuracy and eventually lead to the upgraded POWHEG-V2 `two-rad` version for DY processes; the latter superseeds the previous versions in the POWHEG-V2 framework.

For the purpose of measuring M_W with high accuracy, the results of our study imply that, if tools such as RESBOS or POWHEG-V2 interfaced to "standard" PHOTOS (i.e. with no pair radiation) are used in the measurements, a theoretical systematic uncertainty of some MeV has to be accounted for. This is in agreement with the completely different and independent Tevatron estimate of the theoretical errors of perturbative nature. On the other hand, if more refined and up-to-date generators like POWHEG-V2 `two-rad` interfaced to PHOTOS including pairs are used, the uncertainty due to perturbative contributions is

reduced to the $\sim 1-2$ MeV level. Advances in the field of high-precision calculations and MC generators for DY processes will allow to sustain this expectation.

In summary, our results can serve as a guideline for the assessment of the theoretical systematics at the Tevatron and LHC and allow a more robust precision measurement of the W mass at hadron colliders.

Acknowledgments

This work was supported in part by the Italian Ministry of University and Research under the PRIN project 2010YJ2NYW. AV is supported by the European Commission through the HiggsTools Initial Training Network PITN-GA2012-316704. The work of HM has been supported by the Research Executive Agency (REA) of the European Union under the Grant Agreement number PITN-2010- 264564 (LHCPhenoNet) and is presently supported by the University of Pavia under the grant "Fondo Giovani".

The authors thank the Galileo Galilei Institute for theoretical physics for giving them the possibility of hosting the first meeting of the workshop "W mass measurement at the LHC" (October 2014) and INFN for partial support. They are also grateful to M. Boonekamp, L. Perrozzi and D. Wackeroth for their help in the organization of the meeting.

The authors wish to thank M.L. Mangano for his continuous support of the present study within the CERN LPCC activities.

The authors acknowledge the participation of I. Bizijak to the early stage of this work.

They are indebted to P. Nason for his crucial collaboration in the development of POWHEGv2 with EW corrections and Z. Was for his help in using PHOTOS. They are also grateful to M. Boonekamp, A. Kotwal, L. Perrozzi and D. Wackeroth for continuous encouragement and exchange of information.

The authors wish to thank A. Arbuzov, M.R. D'Alfonso, S. Dittmaier, D. Froidevaux, C. Hays, A. Huss, T. Kurca, C. Oleari, R. Lopes de Sa, C. Schwinn, P. Skands, J. Stark and Z. Was for useful discussions.

FP is grateful to the Mainz Institute for Theoretical Physics (MITP) and to the CERN Theory Unit of the Physics Department for their hospitality and partial support during the development of this work. AV is grateful to the Kavli Institute for Theoretical Physics (KITP) for hospitality and support during the "LHC Run II and the Precision Frontier" supported by NSF PHY11-25915, and to the CERN Theory Unit of the Physics Department for its hospitality and partial support during the development of this work.

Note added in proof

During the completion of this work, we were informed ref. [109] of an effort towards an improved treatment of vector-boson resonances with the POWHEG method, including electroweak corrections. It can be considered as an independent method to perform parton-shower matching for Drell-Yan production of W and Z bosons at the LHC at NLO QCD and NLO electroweak accuracy, as provided by our code POWHEG-V2 `two-rad` developed in the context of the present study. For the future, it would be worthwhile to compare the results of the two approaches.

A Appendix: PHOTOS setup

In this Appendix we detail the input parameter setting used to run PHOTOS:

```
** PHOTOS setup **
-> Version:  3.56
-> Output initializaton screen:
INTERF= 1
ISEC= 0
ITRE= 0
IEXP= 1
IFTOP= 1
IFW= 1
ALPHA_QED= 0.00729735
XPHCUT= 1e-07

Option with interference is active
Option with exponentiation is active EPSEXP=0.0001
Emision in t tbar production is active
Correction wt in decay of W is active

-> Explicit values of flags
phokey_.interf = 1 (interference weight, on by default)
phokey_.isec = 0 (double photon, off by default)
phokey_.ifw = 1 (correction weight in decay of W, on by default)
Photos::meCorrectionWtForW = 0 (ME correction in decay of W, off by default)

-> Setting random seed for each run, using:
srand (time(NULL));
int s1 = rand() % 31327; // (number between 0 and 31327)
int s2 = rand() % 30080; // (number between 0 and 30080)
Photos::setSeed(s1, s2);

-> Setting infrared cutoff for each event, using:

kt2minqed = 0.001d0**2
xphcut = 2d0*sqrt( kt2minqed )/pup(5,3) // pup(5,3):  Invariant mass of decaying
W
Photos::setInfraredCutOff(xphcut);
```

B Appendix: Lepton-pair radiation

In this appendix, we describe how the original PS algorithm implemented in HORACE to simulate photon radiation has been generalized to account for lepton-pair emission in

HORACE-3.1.

In QED the probability that a fermion evolves from a virtuality s_i to s_f emitting photons of energy fraction below a threshold ϵ is given by the Sudakov form factor $\Pi(s_f, s_i)$, describing the so–called "no emission" probability. It can be written as

$$\Pi(s_f, s_i) = \exp\left[-\int_{s_i}^{s_f} \frac{\alpha(s')}{2\pi}\frac{ds'}{s'} I_+\right] \tag{B.1}$$

where

$$I_+ \equiv \int_0^{1-\epsilon} dz\, P(z) = -2\ln\epsilon - \frac{1}{2}(1-\epsilon)^2 - 1 + \epsilon \tag{B.2}$$

and $P(z) = (1+z^2)/(1-z)$ is the unregularized Altarelli–Parisi electron $\to$ electron + photon splitting function. By definition, the Sudakov form factor includes the contribution of virtual and real soft photons to all orders of QED. If we set $\alpha(s) = \alpha(0) \equiv \alpha$, which is the physical value to be used for the electromagnetic coupling constant to describe photon emission, the Sudakov form factor is simply given by

$$\Pi(s_f, s_i) = \exp\left[-\frac{\alpha}{2\pi}\ln\frac{s_f}{s_i} I_+\right] \tag{B.3}$$

that is the formula used in the HORACE default version. If we consider photon radation from a lepton that evolves from $s_i = m^2$ to $s_f \equiv s$, the form factor can be rewritten as

$$\Pi(s, m^2) = \exp\left[-\frac{\alpha}{2\pi}\ln\frac{s}{m^2} I_+\right] \xrightarrow[s\gg m^2]{} \exp\left[-\frac{\beta}{4} I_+\right] \tag{B.4}$$

where $\beta \equiv 2\alpha/\pi\left(\ln s/m^2 - 1\right)$ is the QED collinear factor associated to photon emission from leptons. On the other hand, if we introduce a running electromagnetic coupling constant $\alpha(s)$ as in eq. (3.2) to describe photon emission accompanied by the conversion of photons into lepton pairs, the form factor becomes

$$\Pi(s, m^2) \to \Pi_s(s, m^2) = \exp\left[-\frac{\beta(s)}{4} I_+\right] \tag{B.5}$$

An expansion of the Sudakov form factor $\Pi_s = \epsilon^{-\beta(s)/2}$ up to second order reads

$$\Pi_s \simeq 1 - \frac{\beta(s)}{2}\ln\epsilon + \frac{\beta^2(s)}{8}\ln^2\epsilon + \cdots \tag{B.6}$$

If we consider the dominant contribution of e^+e^- pair emission, one gets for radiating electrons ($f = e$)

$$\beta(s) \simeq \beta_e + \frac{1}{12}\beta_e^2 + \cdots \tag{B.7}$$

by definition of $\beta(s)$ as in the second formula of eq. (3.4) and expansion of the logarithms entering eq. (3.4). In eq. (B.7) $\beta_e \equiv 2\alpha/\pi\left(\ln s/m_e^2 - 1\right)$. Substituting eq. (B.7) in eq. (B.6) gives

$$\Pi_s \simeq 1 - \frac{\beta_e}{2}\ln\epsilon + \frac{\beta_e^2}{8}\ln^2\epsilon - \frac{1}{24}\beta_e^2\ln\epsilon\cdots \tag{B.8}$$

where the second and third term correspond to one and two photon emission and the last one to pair radiation. Therefore, for electrons radiating electron pairs, the ratio between two photon and pair radiation is given by

$$2\gamma/\text{pairs}\,|_{\text{electrons}} \simeq 3\,\ln\epsilon \tag{B.9}$$

On the other hand, by applying the same reasoning to muons ($f=\mu$) emitting e^+e^- pairs, one gets

$$\beta(s) \simeq \beta_\mu + \frac{\mathcal{L}}{12}\,\beta_\mu^2 + \cdots \tag{B.10}$$

where $\beta_\mu \equiv 2\alpha/\pi\left(\ln s/m_\mu^2 - 1\right)$ and $\mathcal{L}$ is a ratio of big logarithms given by

$$\mathcal{L} = \ln\left(\frac{s m_\mu^2}{m_e^4}\right) / \ln\left(\frac{s}{m_\mu^2}\right) \tag{B.11}$$

Note that for $s \simeq M_W^2$ one has $\mathcal{L} \simeq 3$. Now, substitution of eq. (B.10) in eq. (B.6) gives

$$\Pi_s \simeq 1 - \frac{\beta_\mu}{2}\ln\epsilon + \frac{\beta_\mu^2}{8}\ln^2\epsilon - \frac{1}{24}\beta_\mu^2\mathcal{L}\ln\epsilon\cdots \tag{B.12}$$

This implies that for muons radiating electron pairs, the ratio between two photon and pair radiation is enhanced with respect to the electron case and is given by

$$2\gamma/\text{pairs}\,|_{\text{muons}} \simeq \frac{3}{\mathcal{L}}\,\ln\epsilon \simeq \ln\epsilon \tag{B.13}$$

Equation (B.9) and eq. (B.13) explain the results discussed in section 5.1 and section 6.2.

In HORACE-3.1, in addition to the modification of the Sudakov form factor, the treatment of lepton-pair radiation is completed as follows. Because of the meaning of the Sudakov form factor, the number of emitted photons of energy fraction above ϵ inside a sample of N events is given by

$$N_\gamma = (1-\Pi)\,N \tag{B.14}$$

Analogously, the number of emitted photons plus pairs above ϵ is

$$N_\gamma + N_{\text{pairs}} = (1-\Pi_s)\,N \tag{B.15}$$

Therefore, the fraction of emitted pairs ν_{pairs} is given by

$$1 + \nu_{\text{pairs}} = \frac{N_\gamma + N_{\text{pairs}}}{N_\gamma} \tag{B.16}$$

Substituting eq. (B.14) and eq. (B.15) in eq. (B.16) it follows that the fraction of pairs can be cast in the form

$$\nu_{\text{pairs}} = \frac{N_\gamma + N_{\text{pairs}}}{N_\gamma} - 1 = \frac{(1-\Pi_s)N}{(1-\Pi)N} - 1 \tag{B.17}$$

This formula is used in HORACE-3.1 to account for e^+e^- and $\mu^+\mu^-$ pair radiation above ϵ according to the appropriate relative fractions.

References

[1] CDF Collaboration collaboration, T. A. Aaltonen et al., *Precise measurement of the W -boson mass with the Collider Detector at Fermilab*, *Phys.Rev.* **D89** (2014) 072003, [1311.0894].

[2] D0 Collaboration collaboration, V. M. Abazov et al., *Measurement of the W boson mass with the D0 detector*, *Phys.Rev.* **D89** (2014) 012005, [1310.8628].

[3] D0 collaboration, R. Lopes de Sá, *Precise Measurement of the W Boson Mass with the DØ Detector*, *Subnucl. Ser.* **50** (2014) 529–539.

[4] D0 collaboration, H. Li, *Measurement of the W boson mass with the D0 detector*, *Nucl. Part. Phys. Proc.* **273-275** (2016) 2237–2243.

[5] Particle Data Group collaboration, C. Patrignani et al., *Review of Particle Physics*, *Chin. Phys.* **C40** (2016) 100001.

[6] V. Buge, C. Jung, G. Quast, A. Ghezzi, M. Malberti et al., *Prospects for the precision measurement of the W mass with the CMS detector at the LHC*, *J.Phys.* **G34** (2007) N193–N220.

[7] ATLAS Collaboration collaboration, N. Besson, M. Boonekamp, E. Klinkby, S. Mehlhase and T. Petersen, *Re-evaluation of the LHC potential for the measurement of Mw*, *Eur.Phys.J.* **C57** (2008) 627–651, [0805.2093].

[8] CMS collaboration, C. Collaboration, *W-like measurement of the Z boson mass using dimuon events collected in pp collisions at* $\sqrt{s} = 7$ TeV, .

[9] G. Degrassi, P. Gambino and P. P. Giardino, *The* $m_W - m_Z$ *interdependence in the Standard Model: a new scrutiny*, *JHEP* **1505** (2015) 154, [1411.7040].

[10] Gfitter Group collaboration, M. Baak et al., *The global electroweak fit at NNLO and prospects for the LHC and ILC*, *Eur.Phys.J.* **C74** (2014) 3046, [1407.3792].

[11] M. Baak, A. Blondel, A. Bodek, R. Caputo, T. Corbett et al., *Working Group Report: Precision Study of Electroweak Interactions*, 1310.6708.

[12] T. Ježo and P. Nason, *On the Treatment of Resonances in Next-to-Leading Order Calculations Matched to a Parton Shower*, *JHEP* **12** (2015) 065, [1509.09071].

[13] R. Hamberg, W. van Neerven and T. Matsuura, *A Complete calculation of the order* α_s^2 *correction to the Drell-Yan K factor*, *Nucl.Phys.* **B359** (1991) 343–405.

[14] C. Anastasiou, L. J. Dixon, K. Melnikov and F. Petriello, *High precision QCD at hadron colliders: Electroweak gauge boson rapidity distributions at NNLO*, *Phys.Rev.* **D69** (2004) 094008, [hep-ph/0312266].

[15] C. Anastasiou, L. J. Dixon, K. Melnikov and F. Petriello, *Dilepton rapidity distribution in the Drell-Yan process at NNLO in QCD*, *Phys.Rev.Lett.* **91** (2003) 182002, [hep-ph/0306192].

[16] K. Melnikov and F. Petriello, *The W boson production cross section at the LHC through* $O(\alpha_s^2)$, *Phys.Rev.Lett.* **96** (2006) 231803, [hep-ph/0603182].

[17] K. Melnikov and F. Petriello, *Electroweak gauge boson production at hadron colliders through* $\mathcal{O}(\alpha_s^2)$, *Phys.Rev.* **D74** (2006) 114017, [hep-ph/0609070].

[18] R. Gavin, Y. Li, F. Petriello and S. Quackenbush, *W Physics at the LHC with FEWZ 2.1*, *Comput.Phys.Commun.* **184** (2013) 208–214, [1201.5896].

[19] S. Catani, L. Cieri, G. Ferrera, D. de Florian and M. Grazzini, *Vector boson production at hadron colliders: a fully exclusive QCD calculation at NNLO*, *Phys.Rev.Lett.* **103** (2009) 082001, [0903.2120].

[20] R. Boughezal, J. M. Campbell, R. K. Ellis, C. Focke, W. Giele, X. Liu et al., *Color singlet production at NNLO in MCFM*, 1605.08011.

[21] S. Hoeche, Y. Li and S. Prestel, *Drell-Yan lepton pair production at NNLO QCD with parton showers*, 1405.3607.

[22] T. Ahmed, M. Mahakhud, N. Rana and V. Ravindran, *Drell-Yan Production at Threshold to Third Order in QCD*, *Phys. Rev. Lett.* **113** (2014) 112002, [1404.0366].

[23] T. Ahmed, M. K. Mandal, N. Rana and V. Ravindran, *Rapidity Distributions in Drell-Yan and Higgs Productions at Threshold to Third Order in QCD*, *Phys. Rev. Lett.* **113** (2014) 212003, [1404.6504].

[24] D. Wackeroth and W. Hollik, *Electroweak radiative corrections to resonant charged gauge boson production*, *Phys.Rev.* **D55** (1997) 6788–6818, [hep-ph/9606398].

[25] U. Baur, S. Keller and D. Wackeroth, *Electroweak radiative corrections to W boson production in hadronic collisions*, *Phys.Rev.* **D59** (1999) 013002, [hep-ph/9807417].

[26] U. Baur, O. Brein, W. Hollik, C. Schappacher and D. Wackeroth, *Electroweak radiative corrections to neutral current Drell-Yan processes at hadron colliders*, *Phys.Rev.* **D65** (2002) 033007, [hep-ph/0108274].

[27] S. Dittmaier and M. Kramer, *Electroweak radiative corrections to W boson production at hadron colliders*, *Phys.Rev.* **D65** (2002) 073007, [hep-ph/0109062].

[28] U. Baur, S. Keller and W. Sakumoto, *QED radiative corrections to Z boson production and the forward backward asymmetry at hadron colliders*, *Phys.Rev.* **D57** (1998) 199–215, [hep-ph/9707301].

[29] U. Baur and D. Wackeroth, *Electroweak radiative corrections to $p\bar{p} \to W^{\pm} \to \ell^{\pm}\nu$ beyond the pole approximation*, *Phys.Rev.* **D70** (2004) 073015, [hep-ph/0405191].

[30] S. Dittmaier and M. Huber, *Radiative corrections to the neutral-current Drell-Yan process in the Standard Model and its minimal supersymmetric extension*, *JHEP* **1001** (2010) 060, [0911.2329].

[31] A. Arbuzov, D. Bardin, S. Bondarenko, P. Christova, L. Kalinovskaya et al., *One-loop corrections to the Drell-Yan process in SANC. I. The Charged current case*, *Eur.Phys.J.* **C46** (2006) 407–412, [hep-ph/0506110].

[32] A. Arbuzov, D. Bardin, S. Bondarenko, P. Christova, L. Kalinovskaya et al., *One-loop corrections to the Drell–Yan process in SANC. (II). The Neutral current case*, *Eur.Phys.J.* **C54** (2008) 451–460, [0711.0625].

[33] D. Bardin, S. Bondarenko, P. Christova, L. Kalinovskaya, L. Rumyantsev et al., *SANC integrator in the progress: QCD and EW contributions*, *JETP Lett.* **96** (2012) 285–289, [1207.4400].

[34] C. Carloni Calame, G. Montagna, O. Nicrosini and A. Vicini, *Precision electroweak*

calculation of the charged current Drell-Yan process, *JHEP* **0612** (2006) 016, [hep-ph/0609170].

[35] C. Carloni Calame, G. Montagna, O. Nicrosini and A. Vicini, *Precision electroweak calculation of the production of a high transverse-momentum lepton pair at hadron colliders*, *JHEP* **0710** (2007) 109, [0710.1722].

[36] S. Alioli et al., *Precision Studies of Observables in $pp \to W \to \ell\nu$ and $pp \to \gamma, Z \to \ell^+\ell^-$ processes at the LHC*, *Submitted to: Working Group Report* (2016) , [1606.02330].

[37] J. C. Collins, D. E. Soper and G. F. Sterman, *Transverse Momentum Distribution in Drell-Yan Pair and W and Z Boson Production*, *Nucl.Phys.* **B250** (1985) 199.

[38] S. Catani, D. de Florian and M. Grazzini, *Universality of nonleading logarithmic contributions in transverse momentum distributions*, *Nucl.Phys.* **B596** (2001) 299–312, [hep-ph/0008184].

[39] C. Balazs and C. Yuan, *Soft gluon effects on lepton pairs at hadron colliders*, *Phys.Rev.* **D56** (1997) 5558–5583, [hep-ph/9704258].

[40] G. Bozzi, S. Catani, G. Ferrera, D. de Florian and M. Grazzini, *Production of Drell-Yan lepton pairs in hadron collisions: Transverse-momentum resummation at next-to-next-to-leading logarithmic accuracy*, *Phys.Lett.* **B696** (2011) 207–213, [1007.2351].

[41] S. Catani, D. de Florian, G. Ferrera and M. Grazzini, *Vector boson production at hadron colliders: transverse-momentum resummation and leptonic decay*, 1507.06937.

[42] E. Barberio, B. van Eijk and Z. Was, *PHOTOS: A Universal Monte Carlo for QED radiative corrections in decays*, *Comput.Phys.Commun.* **66** (1991) 115–128.

[43] E. Barberio and Z. Was, *PHOTOS: A Universal Monte Carlo for QED radiative corrections. Version 2.0*, *Comput.Phys.Commun.* **79** (1994) 291–308.

[44] P. Golonka and Z. Was, *PHOTOS Monte Carlo: A Precision tool for QED correctio ns in Z and W decays*, *Eur.Phys.J.* **C45** (2006) 97–107, [hep-ph/0506026].

[45] C. Carloni Calame, G. Montagna, O. Nicrosini and M. Treccani, *Higher order QED corrections to W boson mass determination at hadron colliders*, *Phys.Rev.* **D69** (2004) 037301, [hep-ph/0303102].

[46] C. M. Carloni Calame, G. Montagna, O. Nicrosini and M. Treccani, *Multiple photon corrections to the neutral-current Drell-Yan process*, *JHEP* **0505** (2005) 019, [hep-ph/0502218].

[47] G. Bozzi, S. Catani, G. Ferrera, D. de Florian and M. Grazzini, *Transverse-momentum resummation: A Perturbative study of Z production at the Tevatron*, *Nucl.Phys.* **B815** (2009) 174–197, [0812.2862].

[48] S. Frixione and B. R. Webber, *Matching NLO QCD computations and parton shower simulations*, *JHEP* **0206** (2002) 029, [hep-ph/0204244].

[49] P. Nason, *A New method for combining NLO QCD with shower Monte Carlo algorithms*, *JHEP* **0411** (2004) 040, [hep-ph/0409146].

[50] A. Karlberg, E. Re and G. Zanderighi, *NNLOPS accurate Drell-Yan production*, *JHEP* **1409** (2014) 134, [1407.2940].

[51] S. Alioli, C. W. Bauer, C. Berggren, F. J. Tackmann and J. R. Walsh, *Drell-Yan production*

at NNLL′+NNLO matched to parton showers, *Phys. Rev.* **D92** (2015) 094020, [1508.01475].

[52] W. Placzek and S. Jadach, *Multiphoton radiation in leptonic W boson decays*, *Eur.Phys.J.* **C29** (2003) 325–339, [hep-ph/0302065].

[53] T. Sjostrand, S. Mrenna and P. Z. Skands, *PYTHIA 6.4 Physics and Manual*, *JHEP* **0605** (2006) 026, [hep-ph/0603175].

[54] T. Sjostrand, S. Mrenna and P. Z. Skands, *A Brief Introduction to PYTHIA 8.1*, *Comput.Phys.Commun.* **178** (2008) 852–867, [0710.3820].

[55] G. Corcella, I. Knowles, G. Marchesini, S. Moretti, K. Odagiri et al., *HERWIG 6: An Event generator for hadron emission reactions with interfering gluons (including supersymmetric processes)*, *JHEP* **0101** (2001) 010, [hep-ph/0011363].

[56] T. Gleisberg, S. Hoeche, F. Krauss, M. Schonherr, S. Schumann et al., *Event generation with SHERPA 1.1*, *JHEP* **0902** (2009) 007, [0811.4622].

[57] Q.-H. Cao and C. Yuan, *Combined effect of QCD resummation and QED radiative correction to W boson observables at the Tevatron*, *Phys.Rev.Lett.* **93** (2004) 042001, [hep-ph/0401026].

[58] N. E. Adam, V. Halyo, S. A. Yost and W. Zhu, *Evaluation of the Theoretical Uncertainties in the $W \to \ell\nu$ Cross Sections at the LHC*, *JHEP* **0809** (2008) 133, [0808.0758].

[59] N. E. Adam, V. Halyo and S. A. Yost, *Evaluation of the Theoretical Uncertainties in the $Z \to \ell^+\ell^-$ Cross Sections at the LHC*, *JHEP* **05** (2008) 062, [0802.3251].

[60] N. Adam, V. Halyo and S. A. Yost, *Theoretical Uncertainties in Electroweak Boson Production Cross Sections at 7, 10, and 14 TeV at the LHC*, *JHEP* **11** (2010) 074, [1006.3766].

[61] C. Buttar, J. D'Hondt, M. Kramer, G. Salam, M. Wobisch et al., *Standard Model Handles and Candles Working Group: Tools and Jets Summary Report*, 0803.0678.

[62] G. Balossini, G. Montagna, C. M. Carloni Calame, M. Moretti, O. Nicrosini et al., *Combination of electroweak and QCD corrections to single W production at the Fermilab Tevatron and the CERN LHC*, *JHEP* **1001** (2010) 013, [0907.0276].

[63] C. Bernaciak and D. Wackeroth, *Combining NLO QCD and Electroweak Radiative Corrections to W boson Production at Hadron Colliders in the POWHEG Framework*, *Phys.Rev.* **D85** (2012) 093003, [1201.4804].

[64] L. Barzè, G. Montagna, P. Nason, O. Nicrosini and F. Piccinini, *Implementation of electroweak corrections in the POWHEG BOX: single W production*, *JHEP* **1204** (2012) 037, [1202.0465].

[65] L. Barzè, G. Montagna, P. Nason, O. Nicrosini, F. Piccinini et al., *Neutral current Drell-Yan with combined QCD and electroweak corrections in the POWHEG BOX*, *Eur.Phys.J.* **C73** (2013) 2474, [1302.4606].

[66] S. Alekhin et al., *The PDF4LHC Working Group Interim Report*, 1101.0536.

[67] G. Bozzi, J. Rojo and A. Vicini, *The Impact of PDF uncertainties on the measurement of the W boson mass at the Tevatron and the LHC*, *Phys.Rev.* **D83** (2011) 113008, [1104.2056].

[68] G. Bozzi, L. Citelli and A. Vicini, *Parton density function uncertainties on the W boson mass measurement from the lepton transverse momentum distribution*, *Phys.Rev.* **D91** (2015) 113005, [1501.05587].

[69] G. Bozzi, L. Citelli, M. Vesterinen and A. Vicini, *Prospects for improving the LHC W boson mass measurement with forward muons*, 1508.06954.

[70] S. Quackenbush and Z. Sullivan, *Parton distributions and the W mass measurement*, *Phys. Rev.* **D92** (2015) 033008, [1502.04671].

[71] A. Bodek, J. Han, A. Khukhunaishvili and W. Sakumoto, *Using Drell–Yan forward–backward asymmetry to reduce PDF uncertainties in the measurement of electroweak parameters*, *Eur. Phys. J.* **C76** (2016) 115, [1507.02470].

[72] A. V. Konychev and P. M. Nadolsky, *Universality of the Collins-Soper-Sterman nonperturbative function in gauge boson production*, *Phys.Lett.* **B633** (2006) 710–714, [hep-ph/0506225].

[73] CDF collaboration, T. Aaltonen et al., *Precise measurement of the W-boson mass with the CDF II detector*, *Phys.Rev.Lett.* **108** (2012) 151803, [1203.0275].

[74] D0 collaboration, V. M. Abazov et al., *Measurement of the W Boson Mass with the D0 Detector*, *Phys.Rev.Lett.* **108** (2012) 151804, [1203.0293].

[75] CDF, D0 collaboration, T. E. W. Group, *2012 Update of the Combination of CDF and D0 Results for the Mass of the W Boson*, 1204.0042.

[76] A. V. Kotwal and B. Jayatilaka, *Comparison of HORACE and PHOTOS Algorithms for Multiphoton Emission in the Context of W Boson Mass Measurement*, *Adv. High Energy Phys.* **2016** (2016) 1615081, [1510.02458].

[77] N. Davidson, T. Przedzinski and Z. Was, *PHOTOS Interface in C++: Technical and Physics Documentation*, *Comput. Phys. Commun.* **199** (2016) 86–101, [1011.0937v1].

[78] G. Degrassi and A. Vicini, *Two loop renormalization of the electric charge in the standard model*, *Phys. Rev.* **D69** (2004) 073007, [hep-ph/0307122].

[79] S. Actis, A. Ferroglia, M. Passera and G. Passarino, *Two-Loop Renormalization in the Standard Model. Part I: Prolegomena*, *Nucl. Phys.* **B777** (2007) 1–34, [hep-ph/0612122].

[80] S. Actis and G. Passarino, *Two-Loop Renormalization in the Standard Model Part II: Renormalization Procedures and Computational Techniques*, *Nucl. Phys.* **B777** (2007) 35–99, [hep-ph/0612123].

[81] S. Actis and G. Passarino, *Two-Loop Renormalization in the Standard Model Part III: Renormalization Equations and their Solutions*, *Nucl. Phys.* **B777** (2007) 100–156, [hep-ph/0612124].

[82] A. Czarnecki and J. H. Kuhn, *Nonfactorizable QCD and electroweak corrections to the hadronic Z boson decay rate*, *Phys. Rev. Lett.* **77** (1996) 3955–3958, [hep-ph/9608366].

[83] D. Kara, *Corrections of Order $\alpha\alpha_s$ to W Boson Decays*, *Nucl.Phys.* **B877** (2013) 683–718, [1307.7190].

[84] A. Kotikov, J. H. Kuhn and O. Veretin, *Two-Loop Formfactors in Theories with Mass Gap and Z-Boson Production*, *Nucl. Phys.* **B788** (2008) 47–62, [hep-ph/0703013].

[85] W. B. Kilgore and C. Sturm, *Two-Loop Virtual Corrections to Drell-Yan Production at order $\alpha_s\alpha^3$*, *Phys.Rev.* **D85** (2012) 033005, [1107.4798].

[86] R. Bonciani, S. Di Vita, P. Mastrolia and U. Schubert, *Two-Loop Master Integrals for the mixed EW-QCD virtual corrections to Drell-Yan scattering*, 1604.08581.

[87] R. Bonciani, F. Buccioni, R. Mondini and A. Vicini, *Double-real corrections at $O(\alpha\alpha_s)$ to single gauge boson production*, 1611.00645.

[88] D. de Florian, G. F. R. Sborlini and G. Rodrigo, *QED corrections to the Altarelli-Parisi splitting functions*, 1512.00612.

[89] A. Denner, S. Dittmaier, T. Kasprzik and A. Mueck, *Electroweak corrections to W + jet hadroproduction including leptonic W-boson decays*, *JHEP* **0908** (2009) 075, [0906.1656].

[90] A. Denner, S. Dittmaier, T. Kasprzik and A. Mueck, *Electroweak corrections to dilepton + jet production at hadron colliders*, *JHEP* **06** (2011) 069, [1103.0914].

[91] L. Barzè, M. Chiesa, G. Montagna, P. Nason, O. Nicrosini, F. Piccinini et al., *$W\gamma$ production in hadronic collisions using the POWHEG+MiNLO method*, *JHEP* **12** (2014) 039, [1408.5766].

[92] A. Denner, S. Dittmaier, M. Hecht and C. Pasold, *NLO QCD and electroweak corrections to $W + \gamma$ production with leptonic W-boson decays*, *JHEP* **04** (2015) 018, [1412.7421].

[93] A. Denner, S. Dittmaier, M. Hecht and C. Pasold, *NLO QCD and electroweak corrections to $Z + \gamma$ production with leptonic Z-boson decays*, *JHEP* **02** (2016) 057, [1510.08742].

[94] S. Dittmaier, A. Huss and C. Schwinn, *Mixed QCD-electroweak $\mathcal{O}(\alpha_s\alpha)$ corrections to Drell-Yan processes in the resonance region: pole approximation and non-factorizable corrections*, *Nucl.Phys.* **B885** (2014) 318–372, [1403.3216].

[95] S. Dittmaier, A. Huss and C. Schwinn, *$\mathcal{O}(\alpha_s\alpha)$ corrections to Drell-Yan processes in the resonance region*, *PoS* **LL2014** (2014) 045, [1405.6897].

[96] S. Dittmaier, A. Huss and C. Schwinn, *Dominant mixed QCD-electroweak $\mathcal{O}(\alpha_s)$ corrections to Drell–Yan processes in the resonance region*, *Nucl. Phys.* **B904** (2016) 216–252, [1511.08016].

[97] S. Dittmaier, A. Huss and C. Schwinn, *Dominant $\mathcal{O}(\alpha_s\alpha)$ corrections to Drell-Yan processes in the resonance region*, in *Proceedings, 12th International Symposium on Radiative Corrections (Radcor 2015) and LoopFest XIV (Radiative Corrections for the LHC and Future Colliders)*, 2016. 1601.02027.

[98] E. Kuraev and V. S. Fadin, *On Radiative Corrections to e^+e^- Single Photon Annihilation at High-Energy*, *Sov.J.Nucl.Phys.* **41** (1985) 466–472.

[99] O. Nicrosini and L. Trentadue, *Soft Photons and Second Order Radiative Corrections to $e^+e^- \to Z^0$*, *Phys.Lett.* **B196** (1987) 551.

[100] A. Arbuzov, V. Bytev, E. Kuraev, E. Tomasi-Gustafsson and Y. Bystritskiy, *Structure function approach in QED for high energy processes*, *Phys.Part.Nucl.* **41** (2010) 394–424.

[101] M. Skrzypek, *Leading logarithmic calculations of QED corrections at LEP*, *Acta Phys.Polon.* **B23** (1992) 135–172.

[102] S. Jadach, M. Skrzypek and M. Martinez, *Light pair corrections to the Z line shape parameters*, *Phys.Lett.* **B280** (1992) 129–136.

[103] C. Carloni Calame, S. Jadach, G. Montagna, O. Nicrosini and W. Placzek, *Comparisons of the Monte Carlo programs HORACE and WINHAC for single W boson production at hadron colliders*, *Acta Phys.Polon.* **B35** (2004) 1643–1674, [hep-ph/0402235].

[104] S. Alioli, P. Nason, C. Oleari and E. Re, *NLO vector-boson production matched with shower in POWHEG*, *JHEP* **0807** (2008) 060, [0805.4802].

[105] S. Frixione, P. Nason and C. Oleari, *Matching NLO QCD computations with Parton Shower simulations: the POWHEG method*, *JHEP* **0711** (2007) 070, [0709.2092].

[106] T. Ježo, J. M. Lindert, P. Nason, C. Oleari and S. Pozzorini, *An NLO+PS generator for $t\bar{t}$ and Wt production and decay including non-resonant and interference effects*, 1607.04538.

[107] DELPHES 3 collaboration, J. de Favereau et al., *DELPHES 3, A modular framework for fast simulation of a generic collider experiment*, *JHEP* **1402** (2014) 057, [1307.6346].

[108] A. Martin, W. Stirling, R. Thorne and G. Watt, *Parton distributions for the LHC*, *Eur.Phys.J.* **C63** (2009) 189–285, [0901.0002].

[109] A. Mueck and L. Oymanns, "private communication."